



Geoscience BC Report 2020-04

**A geochemical investigation of halogens in spruce treetops
and integration with existing multi-element data –
Blackwater/TREK regions, Central British Columbia
(NTS 093C, 093F).**



By

Colin E. Dunn¹ and David. R. Heberlein²

¹Colin Dunn Consulting Inc., 8756 Pender Park Drive, North Saanich, BC

²Heberlein Geoconsulting, 303-108 West Esplanade, North Vancouver, BC

Table of Contents

Table of Contents	ii
List of Figures	iii
List of Tables	iv
Executive Summary	vi
Introduction.....	1
Previous Studies in BC and Current Project Objectives	1
Relevance to the Exploration Community	4
Survey Area	5
Location and Access	5
Geology.....	5
Surficial Geology.....	5
Bedrock Geology	7
Sampling	9
Analytical Methods.....	10
General.....	10
Sample Preparation	11
Halogen Method Development	11
Quality Control - General	12
Analytical Artifacts and Reanalysis of Selected Samples.....	13
Data Quality	15
Accuracy	15
Precision.....	15
Data Analysis	18
Ash weight vs dry weight equivalent.....	18
Summary Statistics.....	19
Analysis of multi-element results	21

Correlations and principal component analysis	21
Results.....	24
Halogens	24
Fluorine.....	24
Chlorine	28
Bromine	28
Iodine	30
Correlation of halogen anomalies	33
Correlation with pathfinder elements.....	37
Discussion.....	39
Summary and Conclusions	40
Recommendations.....	41
Acknowledgements.....	42
References.....	42

List of Figures

Figure 1. Location of study area within the TREK project, Interior Plateau, central British Columbia.....	3
Figure 2. Sample location map of Jackaman and Sacco (2016), and of this study.	4
Figure 3. Surficial geology and till potential map of the project area (Levson and Giles, 1997; Sacco et al., 2017 a, b and references therein).	6
Figure 4. Generalized geology map of the study area (after Angen et al., 2017).....	8
Figure 5. Spruce-treetop side branch sample collection in central British Columbia, a) showing sampler secured to the helicopter with a safety harness and lanyard; b) detail of sample collection. Photos courtesy of E. Banner taken during the 2015 survey.	10
Figure 6. Gold in spruce needle ash (levelled to dry weight) with sample numbers (data from original survey of Jackaman and Sacco, 2016).....	13
Figure 7. Au and Cu determinations compared to re-analysis of needle ash samples. Values <DL shown as zeros.	15
Figure 8. Log scale charts of data summarized in Table 3 for control vegetation-ash sample VEG-V8a, VEG-4a and CDV-1a.....	17

Figure 9. Histogram showing the variation in ash yield.....	19
Figure 10. Histograms for halogens in ash. One outlier sample (>10,000 ppm Cl) is excluded from the summary statistics.	20
Figure 11. Histograms for halogens – Dry weight equivalent.....	21
Figure 12. Scaled Coordinates (loadings) for PC1 showing a positive association between Fe, Pb, Cs, Rb, Ag, Na and Cu.....	24
Figure 13. Fluorine (ppm: Dry Equiv.) concentration contours over geology (after Angen et al., 2017).	26
Figure 14. Fluorine ppm dry equivalent contours (yellow) over the Analytic Signal magnetic image (Aeroquest, 2014). Dashed white lines show obvious magnetic breaks that are interpreted to be structures. The mapped Blackwater fault is shown by the solid black line in the NE.	27
Figure 15. Chlorine ppm dry equivalent contours over regional geology with geophysical lineaments from Figure 14.	29
Figure 16. Bromine ppm dry equivalent contours over regional geology with geophysical lineaments from Figure 14.	31
Figure 17. Iodine (ppm Dry Equiv.) contours on geology with geophysical lineaments (Figure 14).	32
Figure 18. Tukey Box and Whisker Plots showing variations in halogen concentrations in principal geological units.	33
Figure 19. Summary map showing Br, Cl and I anomalies.....	35
Figure 20. Summary of halogen results showing F ppm dry weight equivalent (red) and contours of a Br-Cl-I summative index (black). The index highlights areas where Cl, Br and I anomalies coincide. Geophysical lineaments from Figure 14.....	36
Figure 21. Areas of coincident PC1 scores (progressive half percentile scaled) and halogen index anomalies. Contours indicate halogen index values; grey dashed lines – lineaments from Analytic Signal magnetic image; solid black line – mapped segment of the Blackwater fault (from Diakow and Levson, 1997). Geology after Angen et al., 2017.	38

List of Tables

Table 1. Average (n = 3) concentrations and method precision (%RSD) obtained for ashed vegetation samples leached with hot de-ionized water. Abbreviations: DL, Detection limit; RSD, Relative standard deviation; wt, Weight.....	12
Table 2. Halogen relative standard deviations (RSD%) for 22 field duplicate pairs.	16

Table 3.	Halogen averages, standard deviations (Std. Dev.) and percentage relative standard deviations (RSD%) for vegetation control samples.	16
Table 4.	Summary Statistics for Halogens in ash and dry weight equivalent concentrations.	20

Executive Summary

In June 2015, spruce branches were collected by helicopter from near the tops of 399 healthy mature interior spruce (a central BC hybrid of white and Engelmann spruce species). The survey followed a 1500 m offset grid pattern covering 1000 km² of the Blackwater River/TREK areas of central British Columbia. Samples were analyzed for 65 elements by ICP-MS and results published by Jackaman and Sacco (2016). There remained a surplus portion of ashed needles from each site. In the current study, these samples were analyzed for the four halogen elements (F, Cl, Br and I) after some further analytical method development at ALS-Geochemistry, North Vancouver.

Experimentation determined that the optimum procedure is to leach 0.5 g of ash in hot de-ionized water and analyze the leachate by a combination of ion chromatography (IC) and inductively coupled plasma mass spectrometry (ICP-MS). Acceptable precision was obtained on repeat analysis of two control ash samples, and detection levels (DL) of 0.002 ppm I, 0.02 ppm Br, 0.05 ppm F and 0.1 ppm Cl were achieved. Field samples yielded concentrations of all four halogens that were well above the limits of analytical detection and with a precision of about 20% relative standard deviation (%RSD) for field duplicate pairs. Precision for blind ash control samples was considerably better at around 5% RSD.

After verification of some of the original trace element data, a reduced data set of 17 of the original 65 elements was combined with the halogens and the correlations determined. Two distinct element associations emerged: 1) Cl-Br-I; and 2) Ag-Br-Cl-Cs-Cu-Na-Pb-Rb.

From a principal component analysis (PCA) of the 17-element dataset (i.e. halogens excluded), the suite of elements that emerged as PC1, and accounted for almost 32% of the data variability, comprised commodity and pathfinder elements which are common to porphyry and epithermal systems - Ag-Cs-Cu-Fe-Na-Pb-Rb.

Fluorine had no statistically significant correlation with any other element. However, when plotted spatially its distribution revealed some distinct trends of which some were coincident with linear magnetic features and known faults. Noteworthy was a series of linear F anomalies with a north-easterly trend crossing the northern half of the survey area. The trend, which is supported by the analytic signal aeromagnetic image and past geological mapping, follows the Blackwater fault and continues for at least 30 km to the SW. It suggests leakage from depth along a broad fault zone.

The other halogens, Br, Cl and I, tend to cluster and, since they are also statistically related, an index of their concentrations was developed. Furthermore, their statistical association with the Ag-Cs-Cu-Fe-Na-Pb-Rb suite provides a guideline toward zones of potential mineralization and possible hitherto unmapped windows through the Chilcotin Group. All three halogens are important ligands for the transport

of metals in hydrothermal fluids. Therefore, coincident anomalies of these elements may be showing areas where there has been hydrothermal activity involving magmatically derived fluids. As such they may represent intriguing exploration opportunities.

Results show that there are areas with Br-Cl-I index anomalies without corresponding metal signatures. Conversely, there are PC1 multi-element anomalies without halogen responses. Most of the latter consist of single sample anomalies scattered over the southern two thirds of the grid. The most curious feature of these anomalies is that they appear to align along two parallel NW-SE trends. The significance of these trends is not known but potentially they reflect structures beneath the volcanic and glacial cover.

Introduction

The halogens (F, Cl, Br and I) are common constituents of igneous, metamorphic and sedimentary rocks (Billings and Williams, 1967). They are particularly enriched in differentiated magmas; the hydrothermal fluids, volatile compounds (mainly in the form of HF, HCl, HBr and HI) and gases derived from them (Aiuppa et al., 2008) play an important role in the mobilization and transport of metals in ore forming systems. In the primary environment, they reside in a variety of hydrous minerals including micas, amphiboles, scapolite, topaz and apatite where F, in particular, can substitute for oxygen and hydroxyl. The heavier halogens Cl, Br and I have larger ionic radii and lower electronegativities than F which favours coordination with large alkali elements. High halogen concentrations are also documented in high salinity liquid phases and tiny mineral phases in fluid inclusions in igneous and hydrothermal minerals (Kendrick et al., 2012; Kendrick and Burnard, 2013). On exposure to surface conditions, these minerals weather and release their halogens as volatile vapours (Br and I) and/or their more stable compounds, or water soluble ions (F and Cl) that disperse to form detectable anomalies in the surficial environment (Trofimov and Rychkov, 2004).

A litho-geochemical study of the wall rocks of intermediate to felsic volcanic-hosted massive sulfide deposits at Crandon, Wisconsin, found that there are fluorine enrichments such that the patterns significantly enlarge the expression of the mineralized zones. Fluorine enrichment extends approximately 320 m into the footwall rocks and at least 220 m into the hanging wall rocks (Lavery, 1985). At the Mac Mo porphyry system in north-central British Columbia (Cope and Spence, 1995) the >5 ppm Mo lies within a broader halo of >500 ppm F. Similar patterns are documented at other porphyry systems, for example at Henderson, Colorado (Seedorff and Einaudi, 2004).

In mineral exploration, there are many case histories that demonstrate positive responses of all these elements and other volatile compounds to zones of concealed mineralization (Al Ajely et al., 1984; Trofimov and Rychkov, 2004) in surficial media. However, the halogens have seen little or no application as pathfinder elements to the exploration for minerals in the extensively drift and volcanic-covered terrains of British Columbia. This is because of their relative difficulty of analysis, a lack of commercially available halogen analytical packages for surficial media, and relatively high cost of analysis.

Previous Studies in BC and Current Project Objectives

In 2005, Geoscience BC sponsored a project entitled “Halogens in Surface Exploration Geochemistry: Evaluation and Development of Methods for Detecting Buried Mineral Deposits” (Dunn et al., 2007). This initial study investigated the optimal analytical procedures available at the time for determining halogen concentrations in soil and vegetation and provided new halogen data from samples collected at

the Mount Polley and QR porphyry deposits, and the 3Ts epithermal prospect in central British Columbia. A recommendation from this study was that since a clear response of labile halogens in soils and vegetation to known mineralization had been established, targets concealed by post-mineralization cover (both glacial and volcanic) needed to be tested and analytical methodology refined. Numerous analytical problems were identified, and it was concluded that further research was required to obtain acceptable precision and accuracy at the low concentration levels in a water leach of soils and vegetation.

A second finding was that halogen signatures vary according to the nature of the mineralization: whereas F may provide the best signature in one area, I or Br may be better in another. This indicates that each style of mineralization is likely to have a different halogen response yet to be clearly defined; hence analysis for all four halogens is advisable.

Bissig et al. (2013) as part of a wider study looking at geochemical responses of blind Cu-Au porphyry-style mineralization beneath Chilcotin Group basalt cover at Woodjam, central B.C., demonstrated that the partial extraction techniques Bioleach and Enzyme Leach produced robust responses in Br and I in soils over blind mineralization at the Three Firs porphyry prospect.

Further studies over two zones of known mineralization on Vancouver Island, the Lara VMS and Mount Washington epithermal prospects, were undertaken by the authors in 2016, aimed at furthering understanding of the processes taking place in the movement and accumulation of the halogens (Heberlein et al., 2017a, 2017b). At the Lara prospect anomalous concentrations of Br and I were coincident with an area of base metal and pathfinder element anomalies in soils and vegetation, but Cl and F patterns suggested a possible outward zonation. A conclusion was that by ashing both organic-rich soils and vegetation prior to analysis the variable interferences introduced by the organic compounds could be circumvented, but further research was required to refine the methodology, especially for F.

In an area of Au mineralization at Mt. Washington, tests involved the collection of soils, transpired fluids and snow. In addition, resin and activated carbon ion collectors were buried in the soil profile for three months to trap volatile emanations from the mineralized zone. In general, the analytical precision for the halogens was fair to poor, but of sufficient quality to relate distribution patterns to zones of known mineralization. There was a clear relationship of halogen enrichments to the zones of known Au mineralization. However, it was considered that further refinement of the analytical technology was required in order to better define distribution patterns of the four halogens and to improve analytical accuracy and precision.

In 2015, Geoscience BC funded a helicopter-supported spruce-treetop sampling program in the Blackwater River area of the TREK project in central British Columbia (Figure 1). Twig and needle

samples were collected on a 1.5 km spaced offset grid and analyzed for a full multi-element suite at Bureau Veritas in Vancouver, BC (Jackaman and Sacco, 2016). The area is forested, has few lakes and a limited road network such that other surface geochemical exploration methods would be impractical.

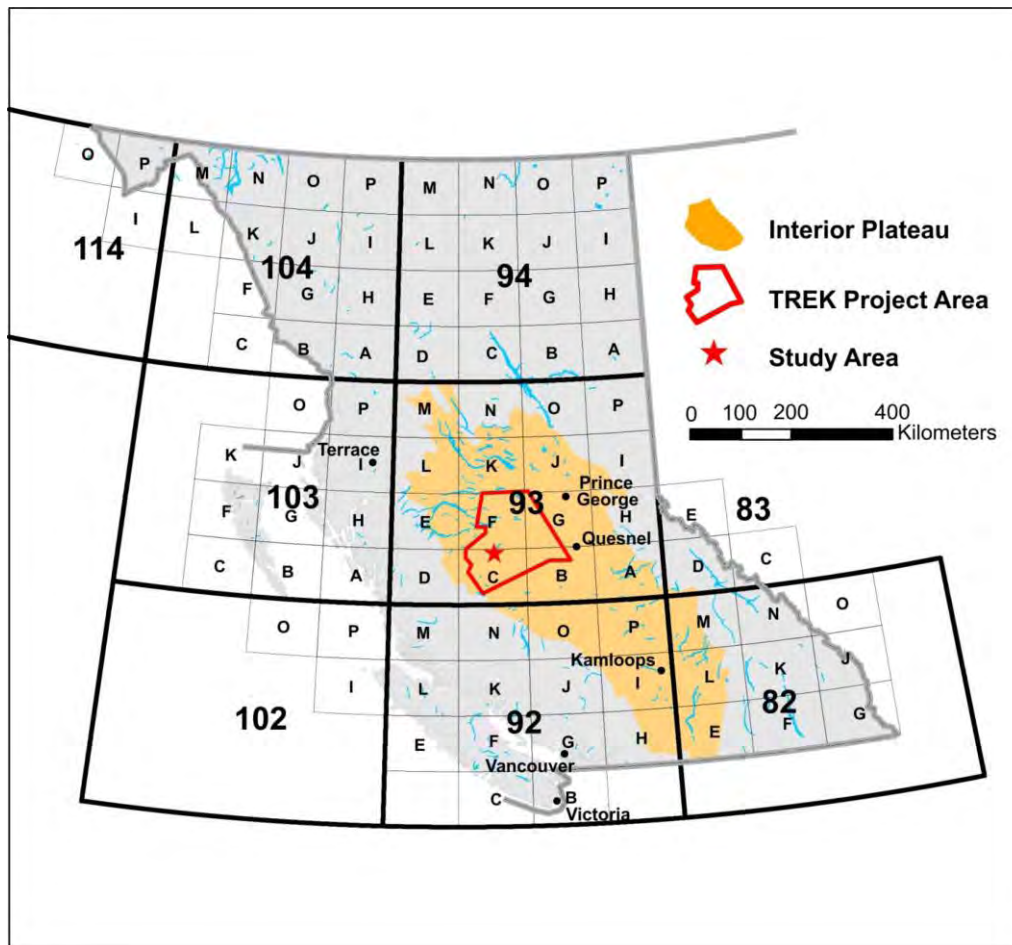


Figure 1. Location of study area within the TREK project, Interior Plateau, central British Columbia.

Jackaman and Sacco (2016) published results from the analysis of 399 milled spruce twig samples (dry tissues) and 22 field duplicates; the needles from these same samples were also analyzed, but were first reduced to ash to concentrate elements prior to multi-element analysis by inductively coupled plasma–mass spectrometry (ICP-MS) after a modified aqua-regia digestion (Bureau Veritas Method VG104-EXT). Sample locations are shown in Figure 2.

Surplus needle ash was available for further analytical work and, since the analysis method for detecting halogens in similar materials was being developed under another project (Heberlein et al., 2017a, b), the opportunity was taken to use the archived samples to further refine the analytical methodology and add another layer of data to the original datasets. The purpose was to examine the distribution patterns of

halogens at a regional scale to determine if these volatile elements might identify geologically meaningful patterns and provide confirmation of some subtle element enrichments identified by the original survey.

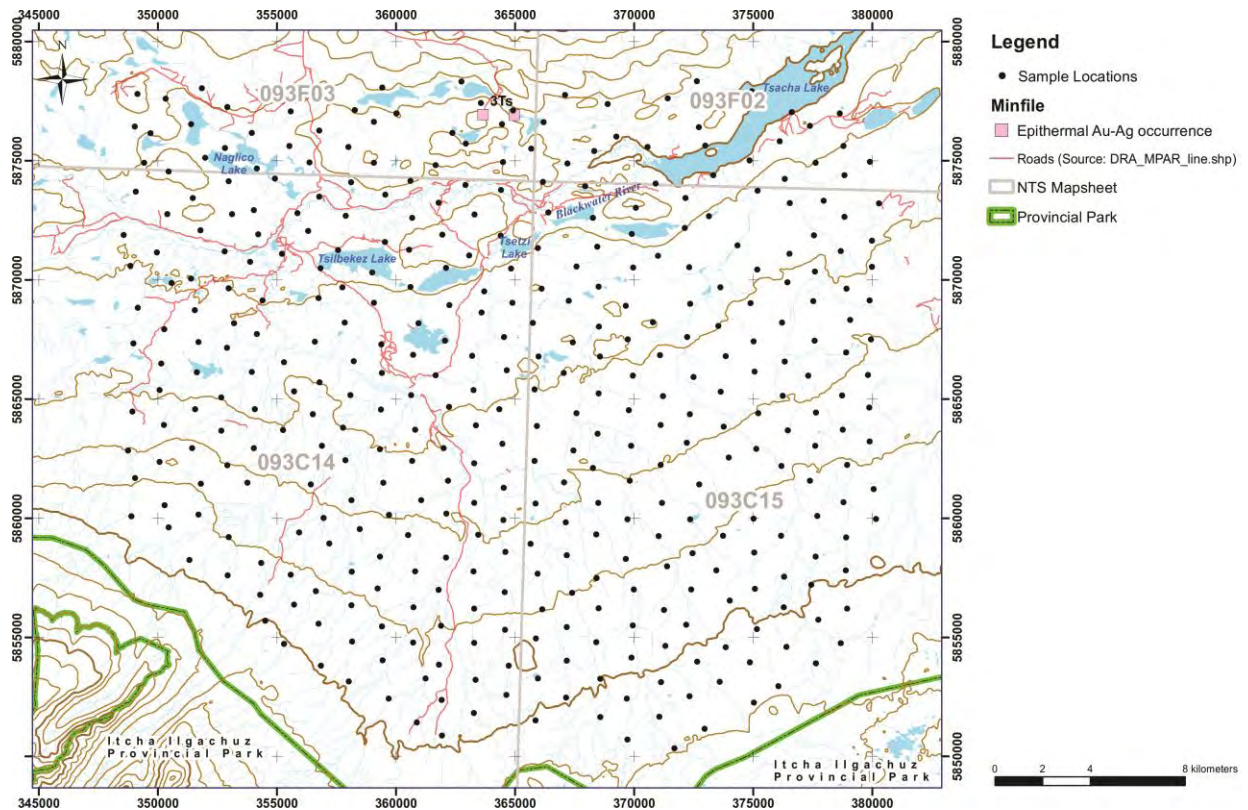


Figure 2. Sample location map of Jackaman and Sacco (2016), and of this study.

Relevance to the Exploration Community

This study is intended to provide the mineral exploration community with an understanding of the potential advantages of determining halogens in tree tissues. It provides exploration companies with knowledge and guidelines about the use of spruce tissues and advice on the appropriate sample digestion and analytical methods to use. This information could contribute to the identification of zones of metal enrichment possibly deriving from covered mineralization as well as revealing structural elements and rock types likely to provide a focus for exploration efforts. This is based on the rationale that the halogen elements are commonly instrumental in the emplacement of metal deposits and, due to their greater mobility in the surficial environment, generate broader haloes of enrichment than the commodity metals themselves. Refinement of the analytical methodology leads to more accurate and precise analytical data, and potential lowering of costs, thus making these methods more attractive and practical to the exploration community.

Survey Area

Location and Access

Jackaman and Sacco (2016) describe the region as a gentle, north-facing slope that is blanketed with glacial drift and dissected by streams flowing into a lowland in the north (Figure 1). Interspersed throughout the 1000 km² survey area are stands of lodgepole pine (*Pinus contorta*), white spruce (*Picea glauca*) and Engelmann spruce (*Picea engelmannii*) of which the latter two are known to hybridize and so are given the generic name of interior spruce. Fortunately, in our experience these spruce species have similar chemical characteristics thus eliminating the need to differentiate between them and their hybrids when sampling. Comparisons of major and trace element concentrations of the two species by the senior author have found no systematic differences, so it is considered that analytical data from the two species and hybrids can be mixed and that the species are interchangeable as sample media.

Wetland features and sedge-grass meadows are common throughout the grid, but interior spruce have a low tolerance to wet substrate conditions resulting in their absence or mal-development in poorly drained areas. Because of this, if a desired sample station proved to be in a bog or wetland, the tissue sample was collected from a tree on drier ground at the margin of the bog, as close as possible to the original station.

Access roads are few and far between over much of the sample grid, but a network of forest service roads is present in the northern third. An abandoned forest service road also crosses the middle of the study area from north to south (Figure 2).

Geology

Surficial Geology

Morainal sediments in the Nechako Plateau region were assigned by Tipper (1971) to the Fraser glaciation, which is dated as Late Wisconsin age (i.e. <15,600 years; Ryder and Clague, 1989). Due to lack of outcrop and poor access, detail of the local Quaternary geology is poorly understood. Sacco et al. (2017a and b) show that much of the study area is covered by ablation till comprised of loose sandy diamicton forming a hummocky surface of small hillocks and hollows. These sediments were deposited near the margins of stagnant ice or in depressions where isolated stagnation occurred. Basal tills are present in the northeast, the south-central and southwest parts of the area, as shown in Figure 3 (after Sacco et al., 2017a and b and the references therein).

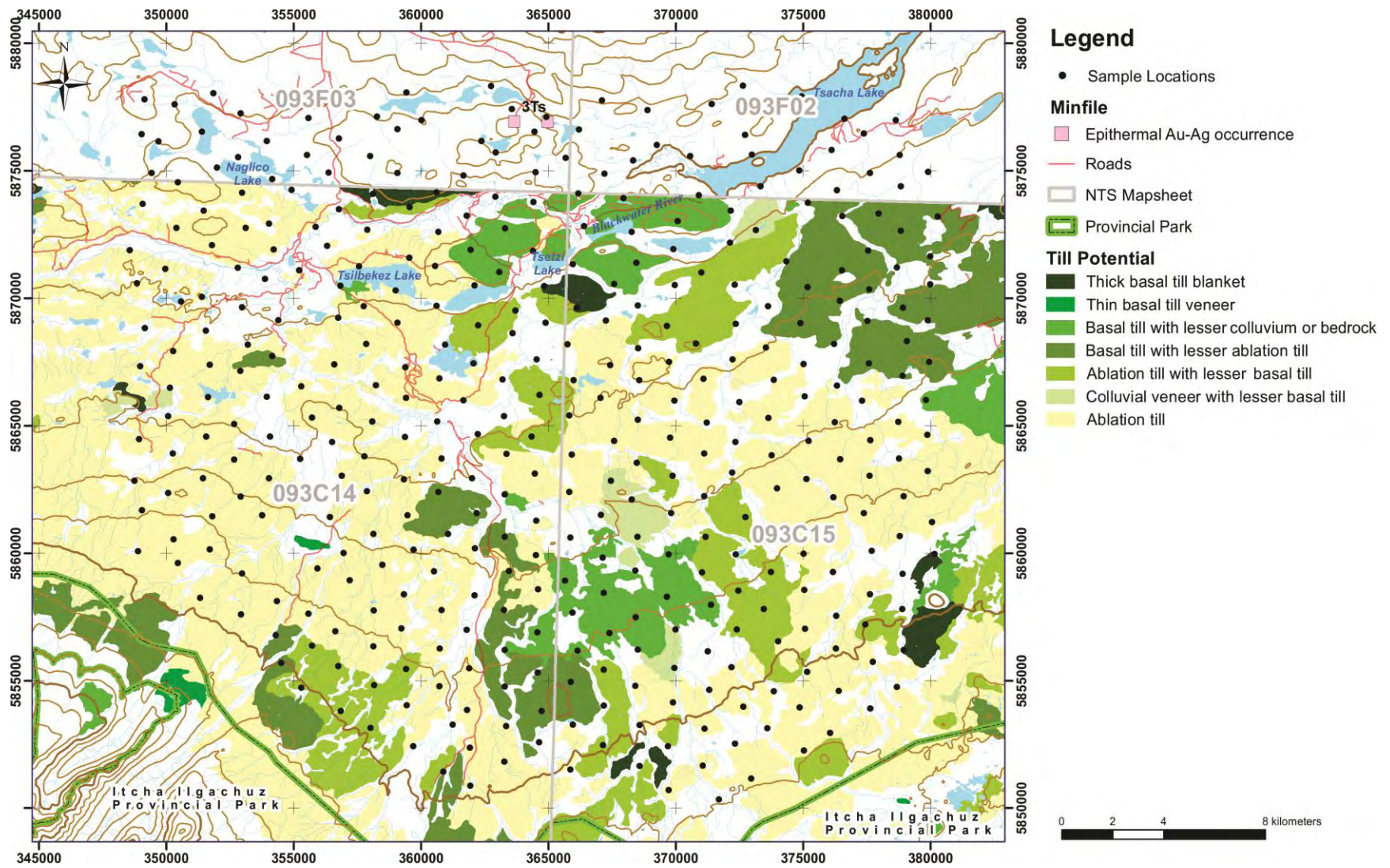


Figure 3. Surficial geology and till potential map of the project area (Levson and Giles, 1997; Sacco et al., 2017 a, b and references therein).

Bedrock Geology

Oligocene to Recent Chilcotin Group basalts form what is mapped as an uninterrupted cover over the southern three quarters of the study area (Dostal et al., 1996; Angen et al., 2017). They are overlain in the southwest corner by mid-Miocene to Holocene-age Anahim volcanic rocks related to the Itcha and Ilgachuz shield volcanoes (Dohaney, 2009). Thickness of the Chilcotin volcanic cover is not known, but mapping by Dohaney (2009) to the southeast of the study area shows that the basalt flows fill topographic lows defined by a paleo-drainage system. Between the paleo-valleys the flows can be very thin or even absent resulting in exposures of older basement rocks as windows through the basalt cover. It is possible that such windows exist beneath the Quaternary glacial sediment cover, which could present opportunities for mineral exploration.

Mesozoic to Paleocene rocks crop out in the north of the area. Oldest units, consisting mostly of volcanics with lesser sediments belonging to the Lower to Middle Jurassic Hazelton Group (Angen et al., 2018), are exposed in the north and northwest parts of the survey area. Bowser Lake Group conglomerates and sandstones overlie the Hazelton Group and form a triangular exposure northwest of Tsetzi Lake and northeast of Tsilbekez Lake. The Bowser Lake Group is intruded by a Late Cretaceous granite north of Tsetzi Lake, which has been classified as part of the Blackwater Suite by Angen et al. (2018). Two north-northwest striking Neogene basalt dykes intrude the Hazelton and Bowser Lake groups east of Tsilbekez lake.

Eocene-age Ootsa Lake Group volcanic rocks consisting mainly of flow banded and spheroidal rhyolite with tuffs and lesser andesite and dacite, crop out to the south of Tsilbekez and Tsetzi lakes and close to the western survey area boundary.

Only two British Columbia MINFILE occurrences, the Tsacha and Tam occurrences, respectively (093F 055 and 093F 068) are known within the study area (Figure 3). Both are low sulphidation epithermal Au-Ag prospects hosted in Hazelton Group rocks that together comprise the 3Ts prospect. Previous biogeochemical studies at the 3Ts prospect established a positive response of halogens to concealed mineralization (Dunn et al., 2007). New Gold's Blackwater intermediate-sulphidation epithermal Au-Ag deposit (MINFILE 093F 037 is located 19 km northeast of the survey area. No recorded mineral occurrences exist within the sampled area south of Blackwater River (flowing west-east between Tsilbekez and Naglico Lakes) where interpretation of airborne geophysics suggests that the underlying bedrock consists exclusively of Chilcotin Group volcanic rocks (Angen et al., 2017; Figure 4).

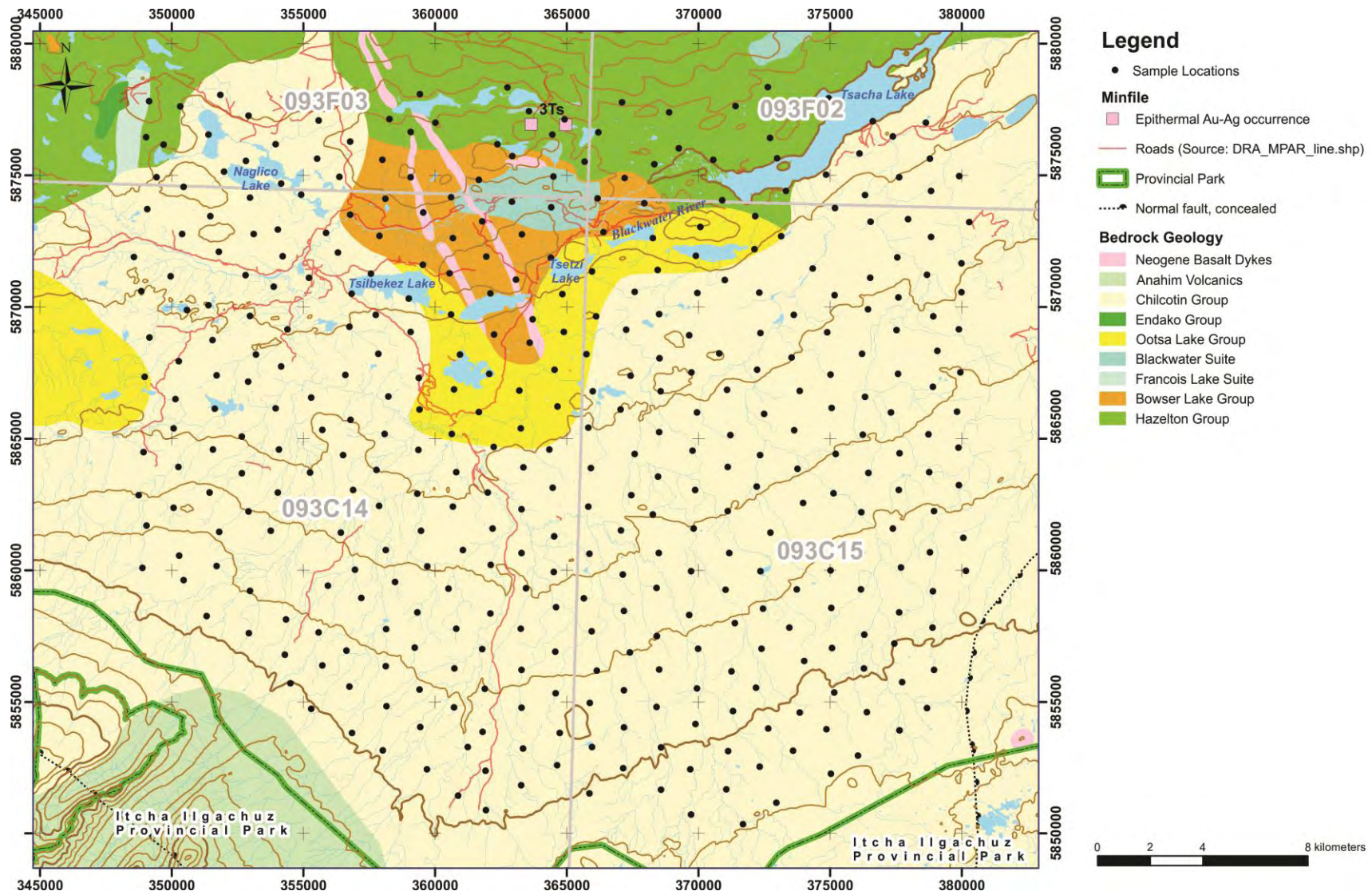


Figure 4. Generalized geology map of the study area (after Angen et al., 2017)

Sampling

Details of the sampling program are given in Jackaman and Sacco (2016), in which it is stated that:

- 1) *“Field survey methods, sample preparation and analysis protocols guiding the 2015 biogeochemical survey were based on previous field surveys, orientation investigations and detailed research (Dunn, 1995, 2007). During a six-day period in June 2015, a 1000 km² area was surveyed using predetermined flight-lines along an offset grid with 1500 m spacing between sample sites. A total of 421 side-branch samples¹ (including 22 field duplicates), each comprising 1 kg of twigs, needles and cones, were systematically collected near the tops of 399 healthy spruce trees (Fig. 5)*
- 2) *The target spruce trees were healthy, 80–100 years old, 20–25 m tall and commonly extended 2–3 m above a lower canopy of lodgepole pine, which typically showed effects of the mountain pine beetle infestation. A recent forest fire in the northern part of the survey area and several immature patches of forest regeneration limited the availability of spruce for a small number of the predetermined sites.*
- 3) *Navigation along the predetermined flight lines and the recording of sample site location coordinates were completed using tablet-based mapping and GPS.”*

¹ collected from just below the crown of the tree (Fig. 5).

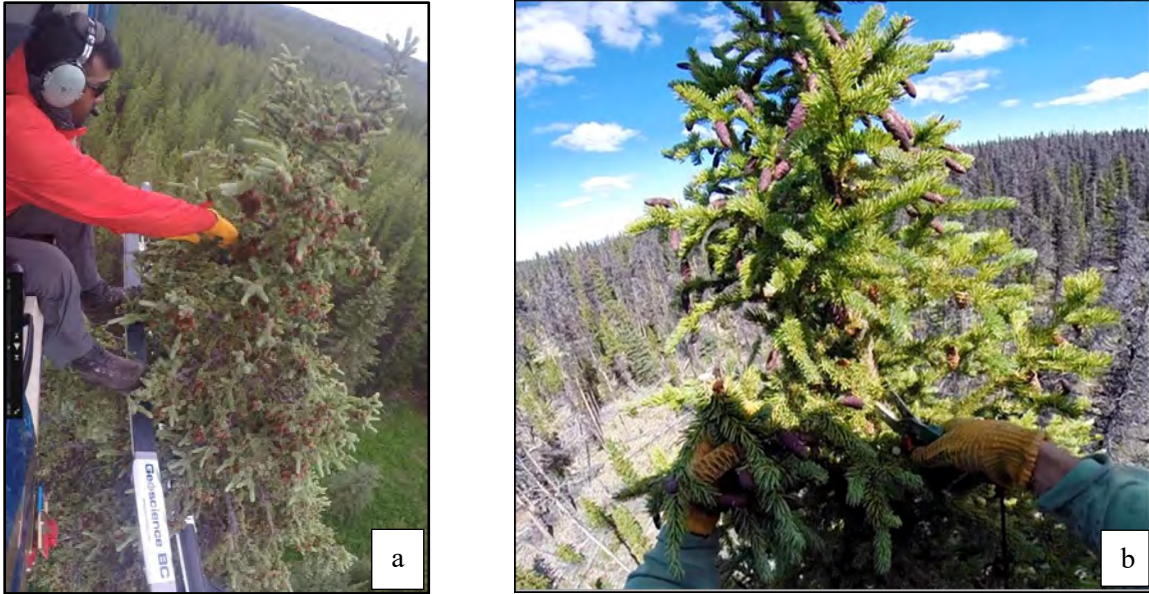


Figure 5. Spruce-treetop side branch sample collection in central British Columbia, a) showing sampler secured to the helicopter with a safety harness and lanyard; b) detail of sample collection. Photos courtesy of E. Banner taken during the 2015 survey.

Analytical Methods

General

Whereas the scientific literature contains many papers dealing with the analysis of volatile elements, most of these involve time-consuming and expensive methods that are beyond the reach of most exploration budgets. For example, Lee et al. (2006) describe a method for quantitative analysis of the halogens F, Cl and Br (but not I) in volatile organo-halogen compounds using Wickbold combustion pre-treatment (Sweester, 1956) in an enclosed system and ion chromatography. They state that:

“the pre-treatment by the Wickbold combustion apparatus makes it possible to burn organic compounds completely in an enclosed system, which can prevent unwanted contamination and loss of volatile halogen elements. The total analysis time was about 50 minutes per sample, which is significantly reduced compared to other methods”.

Since this is an involved, time-consuming, and therefore specialized and expensive method (and does not include I), it tends not to be offered by mainstream commercial laboratories. Most commercial analytical laboratories offer F analysis of inorganic samples by Ion Selective Electrode (ISE) after either a KOH or Na₂O₂ fusion. While appropriate for determination of F and Cl in some types of inorganic samples, for organic samples the ISE method has many potential interferences and detection limits that are too high for the detection of subtle secondary dispersion patterns. Dunn et al. (2007) outline results from a wide

spectrum of methods, and Heberlein et al. (2017a, b) discuss the options for analysis of organic materials and the development of methods for obtaining optimal results. Heberlein et al. (2017b) conclude that:

“Further development of the analytical methods is important if halogens are to become widely used by the mineral exploration community. Work should include further research into low detection limit methods for determining F in organic media [in dry tissue, not just the ash]. This should include further development of the Ion Chromatography (IC) method with the aim of eliminating organic interferences that affect the F chromatogram peaks but should also include assessment of alternative approaches like electro-thermal volatilization-ICP-MS (ETV-ICP-MS) and pyrohydrolysis.”

Sample Preparation

For the original study by Jackaman and Sacco (2016), samples were oven dried at 60°C, the needles removed from the twigs, and a 50 g split of dry needles reduced to ash at 475°C for 24 hours, generating 2–3 g of ash (4-6% ash yield). A 0.25 g aliquot of the ash was analyzed for 64 elements by ICP-MS following aqua-regia digestion. Consequently, enough needle ash remained for this study. The original packets of ash were obtained from W. Jackaman and sent to ALS-Geochemistry, North Vancouver, for further method development, after which all 421 samples were analyzed for F, Cl, Br and I.

Halogen Method Development

‘Super Trace’ F, Cl, Br and I is a recently developed analytical package, which ALS-Geochemistry describes as the ME-HAL01 method. It has proven to be suitable for ashed vegetation (ALS Code for ashing VEG-ASH01), and given the code ME-HAL01a (a different suffix is given for the analysis of halogens in waters - ME-HAL01w) [personal communication, March 2020, Amanda Stoltze, ALS-Geochemistry). Ash samples are leached with hot de-ionized water (90°C) and the leachate analyzed by a combination of ion chromatography (IC) and ICP-MS. Fluorine and Cl are primarily analyzed by IC, with higher concentrations of Cl measured by ICP-MS. Iodine and Br are measured directly by ICP-MS. Previously, following reduction to ash, samples were analyzed for total F by ion-selective electrode (ISE), with a lower detection level of 10 ppm. Significantly lower F detection limits (0.05 ppm F) are now obtainable by the IC method.

Method precision was determined using ashed vegetation tissues (balsam fir needles (V4a) and spruce needles (V8a)). After experimentation at ALS-Geochemistry using both 0.25 g and 0.5 g aliquots of ash it was found that the concentrations and precision for F, Br and I were better using the 0.5 g samples, and so this is the weight that has been adopted throughout this study (Table 1). Interestingly, the Cl results were slightly lower in the 0.5g analyses.

Table 1. Average (n = 3) concentrations and method precision (%RSD) obtained for ashed vegetation samples leached with hot de-ionized water. Abbreviations: DL, Detection limit; RSD, Relative standard deviation; wt., Weight.

Sample	Sample wt	I (ppm)		Br (ppm)		F (ppm)		Cl (ppm)	
		mean	%RSD	mean	%RSD	mean	%RSD	mean	%RSD
Detection limit		0.002		0.02		0.05		0.1	
VEG-V4a	0.25 g	3.85	8.1	67.37	4.8	<DL	<DL	7043	1.85
VEG-V4a	0.50 g	3.99	6	73.5	1.3	14.45	1	6817	0.61
VEG-V8a	0.25 g	0.099	4.8	66.3	1.1	<DL	<DL	4700	4.99
VEG-V8a	0.50 g	0.108	2.8	70.7	1.1	9.76	3.7	4390	0.79

Quality Control - General

Quality control measures included the collection of field duplicate samples (22 pairs) as well as the insertion of ash drift monitor control samples appropriate to the sample media analyzed: a) VEG-V4a - ashed balsam fir needles; b) VEG-V8a - ashed needles from black spruce treetops; c) ashed forest litter (CDV-1a). ALS also used certified reference material OREAS 25a – a mature soil from Australia.

An unacceptably high total measurement error can undermine the ability of a geochemical technique to detect mineralization by obscuring meaningful geochemical patterns (Abzalov, 2008). Sources of total measurement error include a) sampling error; b) preparation and sub-sampling error; and c) analytical error. Errors attributed to each stage of the sampling and analytical process are additive with field sampling error, which is a measure of the representivity of a sample of the material being sampled, accounting for by far the largest proportion of the total.

Total measurement error is expressed as the average percent relative standard deviation (Av %RSD) of the duplicate pairs. It is calculated using the formula:

$$S = \sqrt{(\sum(x-x)^2/N-1)}$$

$$Av \%RSD = \sum(S*100/\bar{x})/N$$

Where S=standard deviation of duplicate pairs, N=number of duplicates, \bar{x} = mean of duplicate pairs.

For the purposes of this study, values of below 20% indicate good data quality; between 20 and 30% acceptable quality; between 30 and 50% marginal quality; and over 50%, poor quality. Elements falling in the marginal and poor categories must be used with caution as their distribution patterns are likely to be influenced by noise caused by poor reproducibility. A discussion of data quality can be found in the results section of this report.

Analytical Artifacts and Reanalysis of Selected Samples

The original multi-element datasets included a comprehensive suite of control samples and duplicate analyses for monitoring analytical quality. These results are detailed in Jackaman and Sacco (2016), who noted that some elements (e.g., Au and Ga in ashed needles) exhibited slightly elevated values along some of the sample sequences. Figure 6 shows a plot of the original Au data with the locations of the original samples and the sample numbers. Analysis of these samples was sequential. The concentrations of these elements were generally very low and may reflect detection-level artifacts related to sample weights and/or heterogeneity. Of concern was a trend of elevated Au values which happens to coincide with the north-easterly glacial dispersion trend and coincidentally, the direction of sampling (Figure 6). However, there is rarely a good relationship between Au in till and Au in vegetation. This is considered to be because traces of Au in the till (commonly in the ppb range) are only selectively transported into a tree such that the signature is commonly too weak to be detected – it appears that a critical mass of an element needs to be present before anomalous concentrations are detected in the tree tissues. This is discussed in Dunn (2007) with an example from the Mt. Milligan porphyry Cu-Au deposit.

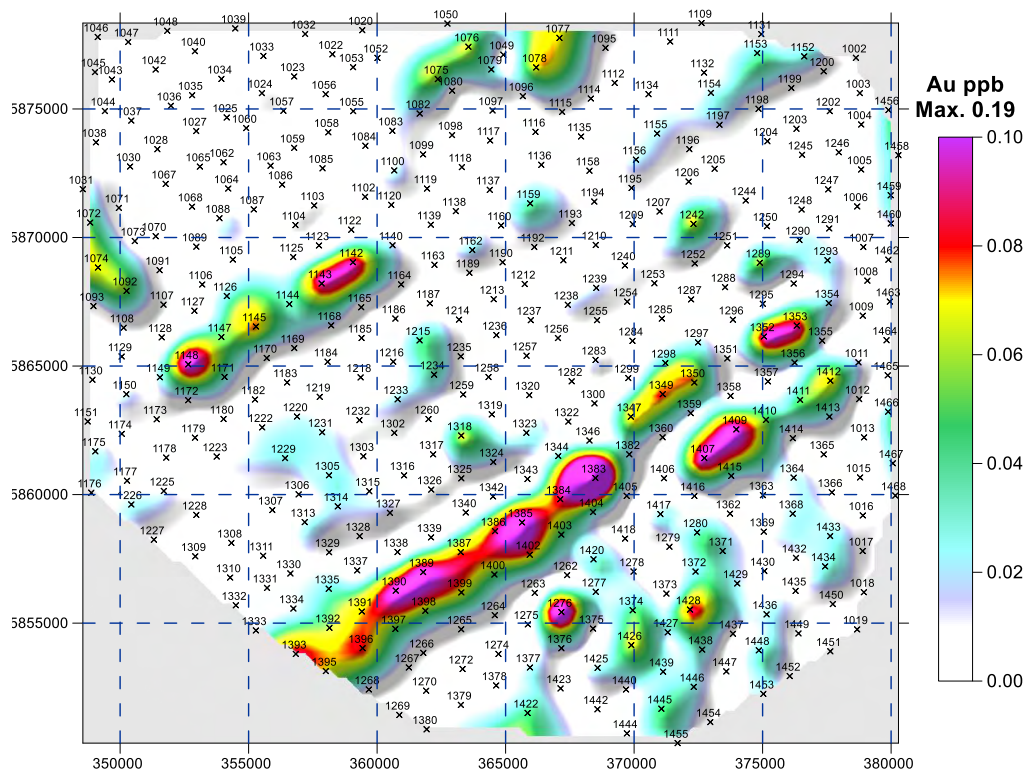


Figure 6. Gold in spruce needle ash (levelled to dry weight) with sample numbers (data from original survey of Jackaman and Sacco, 2016).

Examination of the original data established that the main linear sequence of elevated Au values (sample numbers 1383-1393) was confined to one laboratory test-tube rack, indicating that a slight difference in the digestion procedure (time or temperature) might have been the cause. As a follow-up, the original analytical laboratory (Bureau Veritas Minerals, Vancouver) was asked to re-analyze the ash samples in question to assess the reproducibility of the anomalous results. A total of 22 samples were re-submitted, including two control samples (Table A6, Appendix 1). Results can be summarized as follows:

1. After storage of ash in closed paper packets for 4 years in an unheated basement, the data for most elements were reproducible, confirming that the ash samples retain their integrity over at least several years.
2. The Au results for the problem suite of samples did not reproduce well on reanalysis, however other samples with slightly elevated Au values submitted with them produced similar concentration patterns to the originals, but with generally lower absolute values. The problem samples returned values below the lower detection limit and, consequently, it is recommended that the data for Au (and Te) be disregarded. Similarly, data for Cr and Ga were also non-reproducible and should be similarly excluded from future data interpretations. Furthermore, the results for As and Sb were only poorly reproducible and should not be used. A possible cause for these discrepancies is a hotter than standard digestion, however this could not be confirmed by the laboratory.
3. Other elements that showed a good correlation on re-analysis, but had slightly lower concentrations after 4 years, were Li and Sc, whereas the opposite occurred for Mo (higher after 4 years). However, the patterns were similar (indicating good precision but poor long-term accuracy) so the original data are considered valid for interpretation.

Figure 7 shows examples of the original and repeat analysis of samples that originally showed questionable Au concentrations. Gold values were not reproducible in the suspect sequence, whereas Cu showed excellent repeatability. In fact, most elements reproduced well. Details of all elements are shown in Table A6, Appendix 1. Values <DL show as zeros on the embedded chart (Table A6, Appendix 1). For calculating summary statistics, values below DL (shown in Table A4, Appendix 1), were designated a value of half DL.

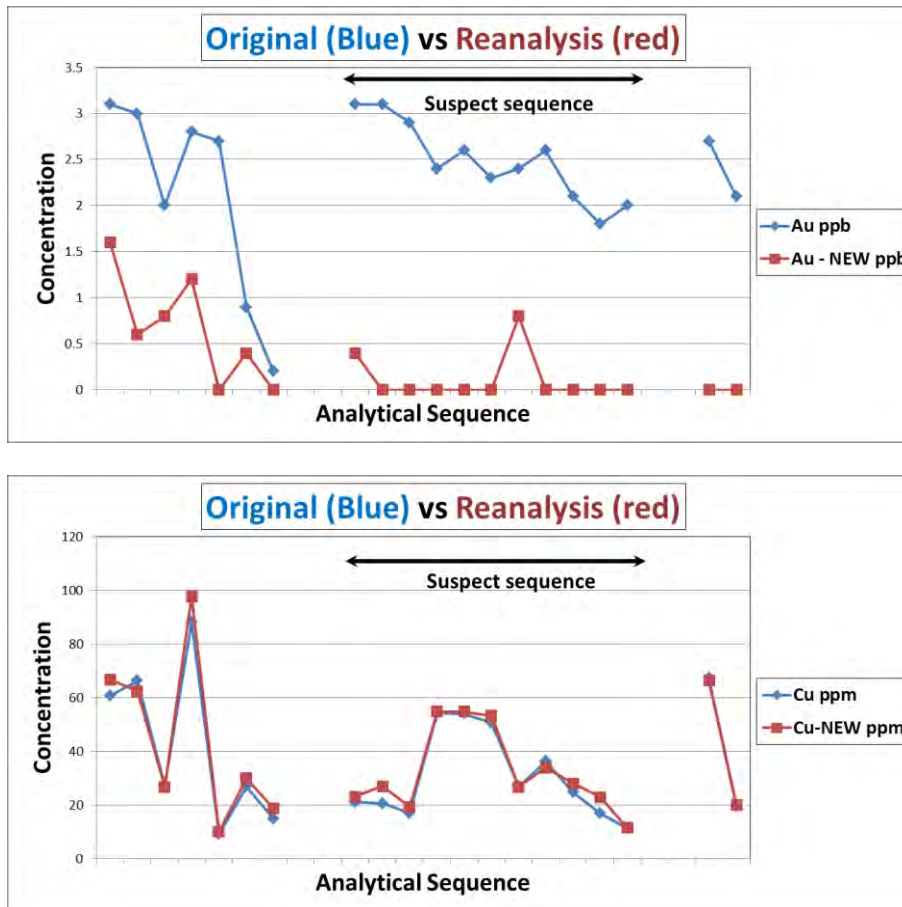


Figure 7. Au and Cu determinations compared to re-analysis of needle ash samples. Values <DL shown as zeros.

Since analytical precision is of more relevance than accuracy for purposes of regional geochemical exploration, we conclude that the original dataset, except for Au, As, Cr, Ga, Sb and Te, is sound for interpretation.

Data Quality

Accuracy

The vegetation ash control samples used are not certified for halogens. No such ash controls are available; hence, these controls cannot be used to monitor the absolute accuracy of the analytical results. Instead, the control results may be used as ‘drift monitors’ to identify systematic errors in the data as well as to estimate the precision of the analytical methods.

Precision

Experimentation was undertaken to refine the analytical methodology for the four halogens; details of the methodology are described in the Analytical Methods section above, with analysis of 0.5 g aliquots

proving to provide better precision than 0.25 aliquots. Full details of the laboratory quality control data are shown in five spreadsheets comprising Table A2 (Appendix 1); Table A3 (Appendix 1) shows all data for the field duplicates.

The reproducibility achieved for analytical duplicate pairs (Table A3, Appendix 1) is summarized in Table 2 and shows that, on average, the relative standard deviation for each of the halogens is about 20%, which is a good to acceptable level for samples from reconnaissance-scale surveys.

In addition to laboratory blanks and soil control OREAS-25a inserted by ALS, two vegetation-ash samples (VEG-V8a and VEG-V4a) were also included in each analytical batch (Table A2, Appendix 1). The precision on all these controls was very good and somewhat better than that of the blind control CDV-1a, because the latter proved to have, in particular, lower concentrations of F than either the survey samples or laboratory controls. Table 3 shows the results for the three vegetation controls (depicted also in Figure 8) which mostly yielded better analytical precision than the field duplicates.

Table 2. Halogen relative standard deviations (RSD%) for 22 field duplicate pairs.

Average RSD% (n=22 pairs)				
Analyte	Br	Cl	F	I
Average RSD	19.8%	20.3%	16.8%	17.9%

Table 3. Halogen averages, standard deviations (Std. Dev.) and percentage relative standard deviations (RSD%) for vegetation control samples.

Control VEG-V8a: n=12	I	Br	F	Cl
Average (ppm)	0.14	53.87	12.77	3888
Std Dev.	0.01	2.65	0.53	417
RSD%	6.1	4.9	4.2	10.7
Control VEG-V4a: n=5				
Average (ppm)	4.3	57	17	5838
Std Dev.	0.15	3.17	0.72	665
RSD%	3.5	5.6	4.2	11.4
Control CDV-1a: n=24				
Average (ppm)	0.11	94.48	8.14	395
Std. Dev.	0.01	3.57	5.91	23
RSD%	9.2	3.8	72.7	5.7

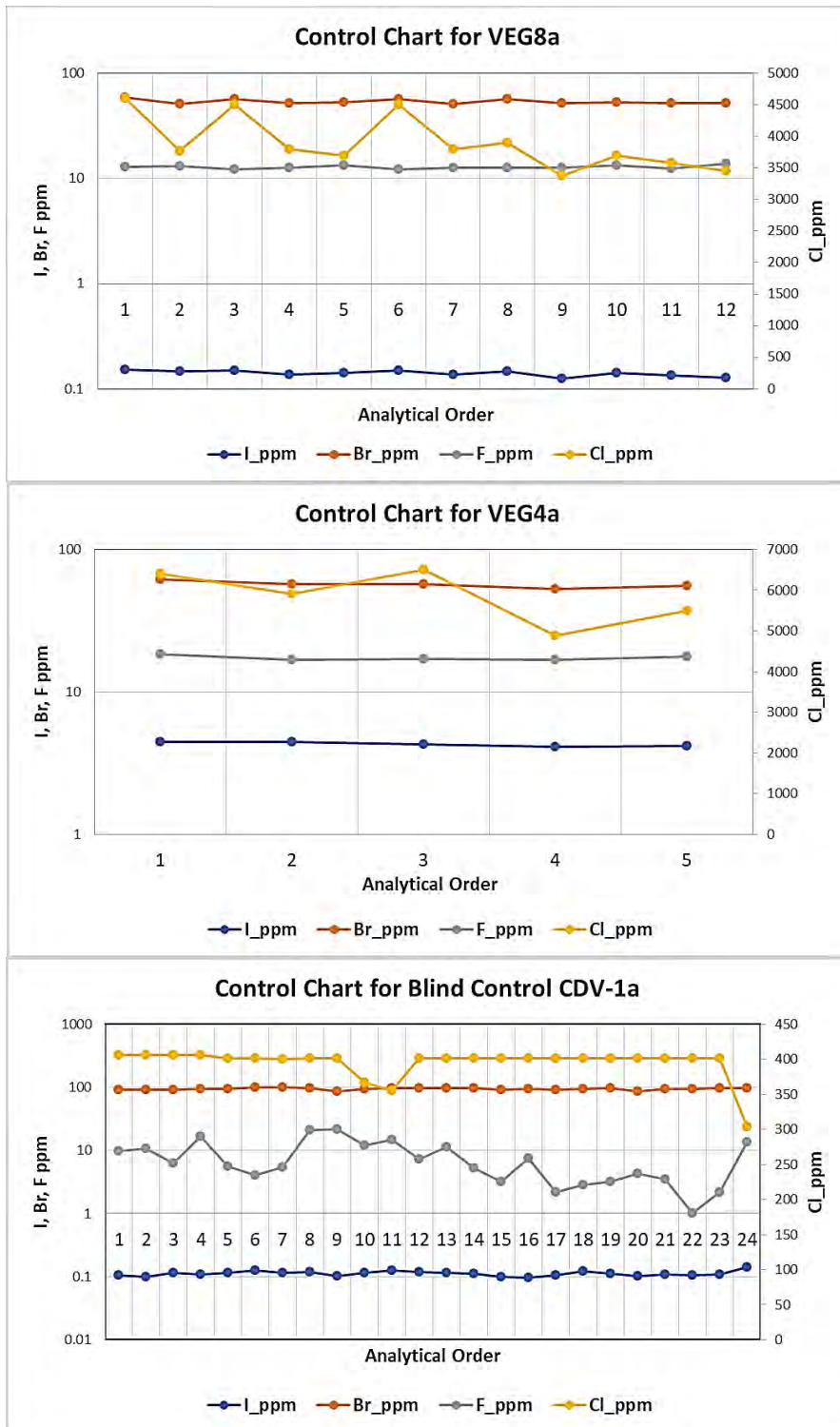


Figure 8. Log scale charts of data summarized in Table 3 for control vegetation-ash sample VEG-V8a, VEG-4a and CDV-1a.

Data Analysis

Ash weight vs dry weight equivalent

Prior to plotting the spatial distributions and inter-element relationships of the analytical results, the data were first levelled to dry weight equivalent values, to take into account variations in the ash yields (Table A4, Appendix 1). Levelling is accomplished by taking the ash yield x element concentration in ash and dividing it by 100. The median yield was 3.68% and the mean was 3.80% with a few outliers. Variation in ash yield is a common phenomenon in biogeochemical datasets, especially from a large survey. A histogram showing of ash yields is shown in Figure 9. Possible reasons for these variations include:

1. Natural variations due to age of growth, needle density, and variable health of the trees;
2. Aspect, with relation to topography and sun exposure (although unlikely in this survey, given the overall flatness of the land) and the fact that samples were from treetops, not the lower limbs;
3. Substantial differences in elevation. This is not the case in the low relief survey area from which the samples were collected. The land slopes gently to the north with a maximum elevation change of 500m from south to north across the sample grid; there is no systematic variation in ash yield with elevation;
4. Drainage conditions: interior spruce cannot tolerate wet and boggy conditions; however sampling was carried out on relatively dry ground outside of the boggy areas.
5. Contamination by airborne dust can be a problem in certain areas close to unpaved roads and mine sites, but not in the pristine conditions of this remote area:
6. Possible hybridization of the two spruce species - a feature that would not be possible to detect without genetic coding, hence standard practice in this part of British Columbia is to refer to the two species collectively as interior spruce.

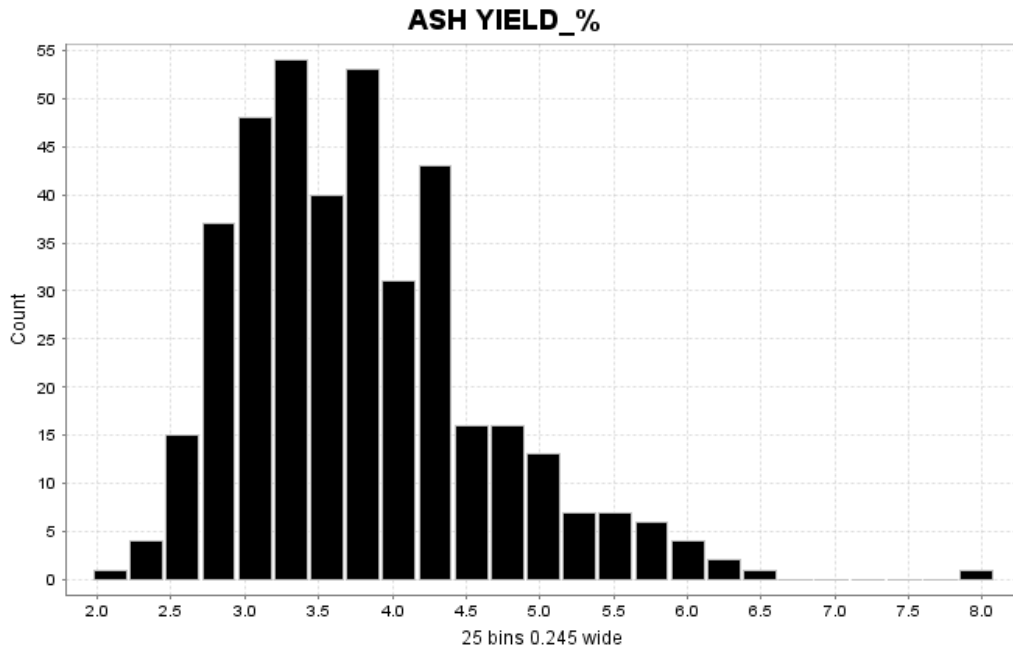


Figure 9. Histogram showing the variation in ash yield.

In the event that ashing was incomplete, traces of charcoal would remain in the ash adding to the apparent ash yield. However, examination of oven standard results (used to monitor the completeness of ashing) showed no indication of incomplete ashing: the oven standard ash yield range was from 2.52 to 2.63% (data from Jackaman and Sacco, 2016).

In practice the difference in distribution patterns of elements in ash and in dry-equivalent data are minor. A detailed discussion of ashing is given in Dunn (2007), with additional references.

Summary Statistics

Summary statistics for the halogen results are presented in Table 4. Only one sample yielded a non-detectable value for F in ash (<0.5 ppm F) with the remainder containing from 15-324 ppm. This sample (Sample ID 1012) on further examination is concluded to be an analytical artifact and thus its F value is excluded from the summary statistics and maps. For Cl there was a remarkable range from 0.1 to >10000 ppm in ash. Iodine and Br each show an order of magnitude lower range of concentrations from F and Cl. Histograms of halogen concentrations are shown in Figure 10 (for ash) and Figure 11 (dry equivalent values).

Table 4. Summary Statistics for Halogens in ash and dry weight equivalent concentrations.

	F_ppm_Ash	F_ppm Dry Eq.	Cl_ppm_Ash	Cl_ppm Dry Eq.	Br_ppm_Ash	Br_ppb Dry Eq.	I_ppm_Ash	I_ppm Dry Eq.
Count Numeric	398	398	399	399	399	399	399	399
Minimum	15.25	0.50	0.05	0.0	0.05	2.3	0.001	0.04
Maximum	324	11.47	10001	>437.4	71	2694.8	0.212	9.92
Mean	61.76	2.33	926	31.8	2.9	105.5	0.034	1.23
Median	52.60	2.01	507	19.7	1.2	43.7	0.023	0.86
Range	323.98	11.47	10001	>437.4	71.0	2692.5	0.211	9.88
Interquartile Range	38.60	1.71	1230	41.3	1.8	61.8	0.029	0.97
Standard Deviation	37.881	1.442	1144	40.317	6.074	227.505	0.0292	1.0771
25 percentile	36.40	1.30	100	4.1	0.4	15.7	0.014	0.55
50 percentile	52.60	2.01	507	19.7	1.2	43.7	0.023	0.86
75 percentile	75.00	3.01	1330	45.4	2.3	77.6	0.043	1.52
90 percentile	103.50	4.09	2360	81.2	7.8	269.6	0.073	2.63
95 percentile	133.00	4.92	2940	96.8	13.9	502.2	0.091	3.28
99 percentile	193.50	8.22	5400	181.5	29.7	1114.1	0.146	4.95

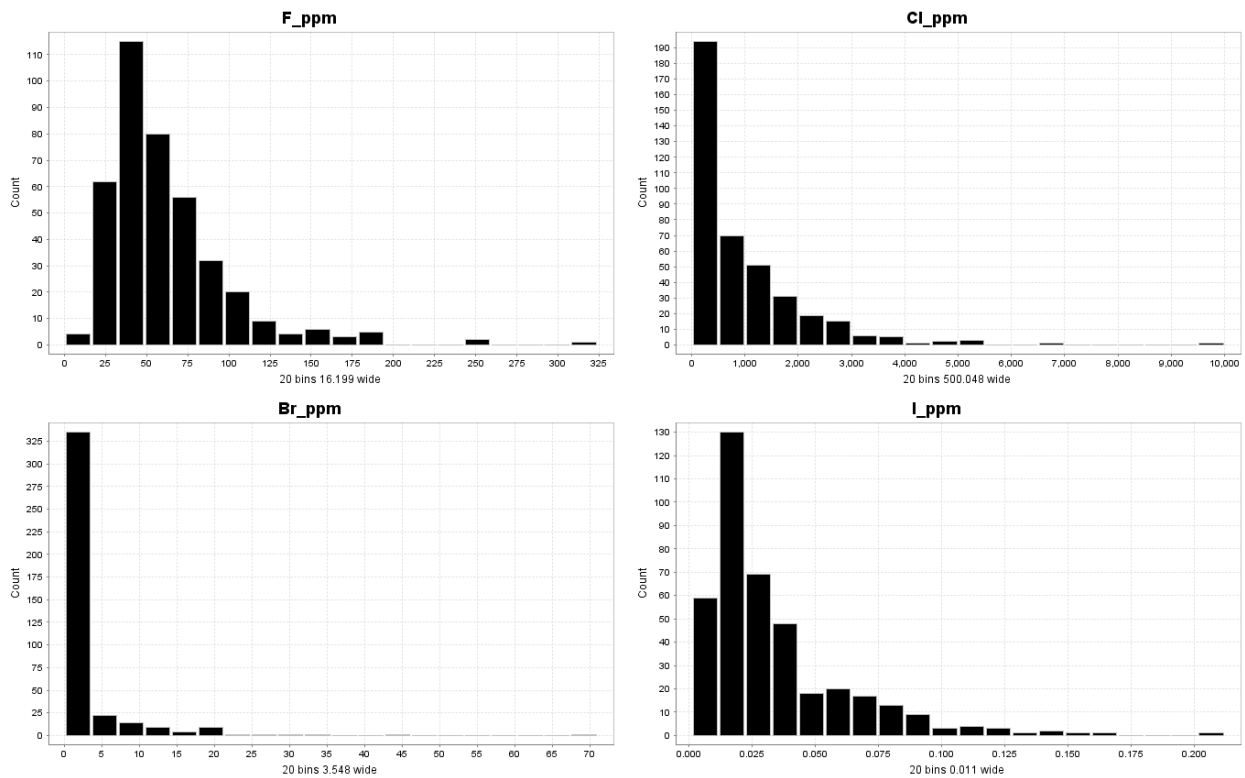


Figure 10. Histograms for halogens in ash. One outlier sample (>10,000 ppm Cl) is excluded from the summary statistics.

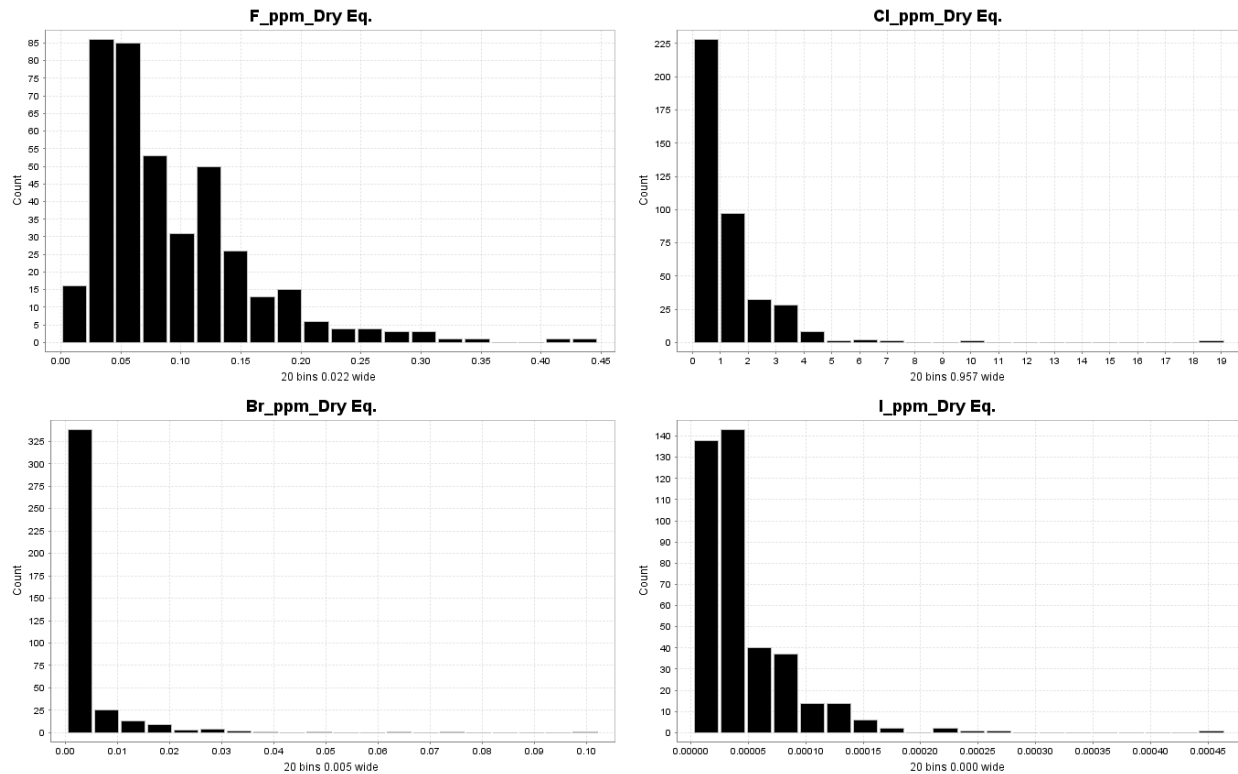


Figure 11. Histograms for halogens – Dry weight equivalent.

Analysis of multi-element results

One objective of this study is to assess the value of halogens in vegetation as regional scale indicators of mineralization. To do this, the halogen results are compared to the original multi-element dataset of Jackaman and Sacco (2016). As discussed above, the poor data quality for some of those elements means that they could not be included in this analysis. Therefore, the suite of pathfinder elements with adequate data quality available for interpretation is somewhat limited. Furthermore, also excluded from this analysis are: 1) elements that failed our QC screening (e.g. Au, As, Ga, Cr, Sb and Te); or 2) elements with interquartile ranges of zero; or 3) elements with high-end or low-end truncation due to concentrations exceeding upper or lower detection limits. Consequently, the list of elements considered for the data analysis was distilled to 17 (mostly commodity and pathfinder elements plus the four halogens - Table 7).

Correlations and principal component analysis

A correlation matrix of the remaining elements is shown in Table 7. Pairs with a significant correlation coefficient (defined as $r \geq 0.4$)² are highlighted in red. Each of the highlighted element pairs have been

² Defined using a significant level of r table and examination of histograms.

validated with scatter plots to ensure that no false correlations are considered. The correlation matrix shows positive correlations for the halogens Br Cl, and I as well as positive correlations for several commodity element pairs.

A principal components analysis was carried out in the software program ioGAS™ on the same element suite, minus the halogens, to investigate element associations within the pathfinder element suite. A Box-Cox transformation with a 2% trim was used to exclude outlier values. Four principal components (PCs) with Eigenvalues >1 were extracted. Eigen values and cumulative percentage of the variance explained by each PC are presented in Table 6.

Table 6. Eigenvalues and cumulative percent of variance explained for the first four Principal components.

	<u>Eigenvalues</u>	<u>Percent</u>	<u>Cumulative %</u>
PC1	5.41	31.82	31.82
PC2	2.856	16.8	48.62
PC3	1.236	7.27	55.89
PC4	1.129	6.643	62.53

Scaled coordinates (loadings) for the PC's are presented in Table 8 and shown graphically for PC1 in Figure 12.

PC1 confirms the results of the correlation matrix and defines an element suite of Ag-Cs-Cu-Fe-Na-Pb-Rb at a loading of >0.5. This suite of elements contains commodity and pathfinder elements common to porphyry and epithermal systems. Results are discussed in the next section. PC2 containing Ba, Co and Ni, is possibly indicative of the Chilcotin basalt composition, which is widespread in the survey area. Except for Zn in PC3, none of the elements have a particularly strong influence on the last two principal components. Therefore, the following discussion will concentrate on the PC1 results only.

Table 7. Pearson correlation matrix of Log (10) transformed values showing positive correlations (red) significant at the 95% confidence level.

Correlation - 399

rows - Pair - Log 10	I_ppm	Br_ppm	F_ppm	Cl_ppm	Ag_ppb	B_ppm	Ba_ppm	Cd_ppm	Co_ppm	Cs_ppm	Cu_ppm	Fe_pct	Li_ppm	Mo_ppm	Na_pct	Ni_ppm	Pb_ppm	Rb_ppm	S_pct	Sr_ppm	Zn_ppm
I_ppm	1	0.58	0.14	0.53	0.26	-0.018	0.065	0.021	0.18	0.32	0.39	0.14	-0.023	0.11	0.15	0.19	0.28	0.34	0.079	-0.21	0.086
Br_ppm	0.58	1	-0.075	0.66	0.35	0.016	0.066	0.051	0.22	0.42	0.46	0.17	0.03	0.16	0.31	0.15	0.36	0.39	0.083	-0.16	0.054
F_ppm	0.14	-0.075	1	-0.24	-0.086	-0.17	0.096	-0.061	0.0091	-0.13	-0.17	-0.1	-0.031	-0.099	-0.28	-0.037	-0.092	-0.15	-0.11	0.06	-0.041
Cl_ppm	0.53	0.66	-0.24	1	0.53	0.25	-0.07	0.15	0.21	0.52	0.65	0.29	0.19	0.33	0.66	0.17	0.46	0.53	0.18	-0.3	0.13
Ag_ppb	0.26	0.35	-0.086	0.53	1	0.3	-0.081	0.35	0.26	0.47	0.7	0.31	0.15	0.32	0.51	0.21	0.52	0.53	0.31	-0.19	0.27
B_ppm	-0.018	0.016	-0.17	0.25	0.3	1	-0.25	0.13	-0.077	0.19	0.38	0.26	0.33	0.3	0.55	-0.01	0.13	0.19	0.17	-0.22	0.059
Ba_ppm	0.065	0.066	0.096	-0.07	-0.081	-0.25	1	0.11	0.27	0.05	-0.09	-0.39	-0.52	-0.44	-0.25	0.21	-0.06	-0.0066	-0.21	0.54	0.21
Cd_ppm	0.021	0.051	-0.061	0.15	0.35	0.13	0.11	1	0.3	0.26	0.34	0.14	-0.044	-0.039	0.25	0.21	0.48	0.32	0.21	-0.065	0.2
Co_ppm	0.18	0.22	0.0091	0.21	0.26	-0.077	0.27	0.3	1	0.35	0.33	0.01	-0.12	-0.059	0.23	0.54	0.17	0.45	0.04	-0.075	0.2
Cs_ppm	0.32	0.42	-0.13	0.52	0.47	0.19	0.05	0.26	0.35	1	0.58	0.22	-0.013	0.033	0.51	0.18	0.44	0.68	0.29	-0.28	0.077
Cu_ppm	0.39	0.46	-0.17	0.65	0.7	0.38	-0.09	0.34	0.33	0.58	1	0.39	0.078	0.26	0.6	0.38	0.5	0.73	0.4	-0.3	0.33
Fe_pct	0.14	0.17	-0.1	0.29	0.31	0.26	-0.39	0.14	0.01	0.22	0.39	1	0.34	0.42	0.39	-0.021	0.34	0.18	0.32	-0.31	0.0073
Li_ppm	-0.023	0.03	-0.031	0.19	0.15	0.33	-0.52	-0.044	-0.12	-0.013	0.078	0.34	1	0.5	0.34	-0.16	0.12	-0.039	0.083	-0.35	-0.13
Mo_ppm	0.11	0.16	-0.099	0.33	0.32	0.3	-0.44	-0.039	-0.059	0.033	0.26	0.42	0.5	1	0.33	-0.16	0.15	0.022	0.014	-0.28	0.079
Na_pct	0.15	0.31	-0.28	0.66	0.51	0.55	-0.25	0.25	0.23	0.51	0.6	0.39	0.34	0.33	1	0.21	0.41	0.52	0.28	-0.41	0.041
Ni_ppm	0.19	0.15	-0.037	0.17	0.21	-0.01	0.21	0.21	0.54	0.18	0.38	-0.021	-0.16	-0.16	0.21	1	0.099	0.48	0.12	-0.082	0.3
Pb_ppm	0.28	0.36	-0.092	0.46	0.52	0.13	-0.06	0.48	0.17	0.44	0.5	0.34	0.12	0.15	0.41	0.099	1	0.36	0.31	-0.17	0.11
Rb_ppm	0.34	0.39	-0.15	0.53	0.53	0.19	-0.0066	0.32	0.45	0.68	0.73	0.18	-0.039	0.022	0.52	0.48	0.36	1	0.29	-0.22	0.29
S_pct	0.079	0.083	-0.11	0.18	0.31	0.17	-0.21	0.21	0.04	0.29	0.4	0.32	0.083	0.014	0.28	0.12	0.31	0.29	1	-0.25	-0.0051
Sr_ppm	-0.21	-0.16	0.06	-0.3	-0.19	-0.22	0.54	-0.065	-0.075	-0.28	-0.3	-0.31	-0.35	-0.28	-0.41	-0.082	-0.17	-0.22	-0.25	1	0.16
Zn_ppm	0.086	0.054	-0.041	0.13	0.27	0.059	0.21	0.2	0.2	0.077	0.33	0.0073	-0.13	0.079	0.041	0.3	0.11	0.29	-0.0051	0.16	1

Table 8. Scaled coordinates (loadings) for the first four principal components.

Scaled Coordinates	PC1	PC2	PC3	PC4
Ag_ppb	0.764	0.099	0.211	0.190
B_ppm	0.484	-0.341	0.212	-0.011
Ba_ppm	-0.282	0.752	0.150	0.133
Cd_ppm	0.459	0.314	0.019	0.382
Co_ppm	0.387	0.550	-0.035	-0.413
Cs_ppm	0.687	0.269	-0.277	0.048
Cu_ppm	0.868	0.173	0.094	0.012
Fe_pct	0.577	-0.394	0.006	0.095
Li_ppm	0.401	-0.635	0.156	-0.145
Mo_ppm	0.383	-0.581	0.437	-0.120
Na_pct	0.792	-0.145	-0.029	-0.134
Ni_ppm	0.374	0.562	-0.010	-0.484
Pb_ppm	0.662	0.074	-0.069	0.477
Rb_ppm	0.740	0.392	-0.089	-0.157
S_pct	0.477	-0.046	-0.417	0.296
Sr_ppm	-0.480	0.395	0.400	0.347
Zn_ppm	0.273	0.333	0.689	0.002

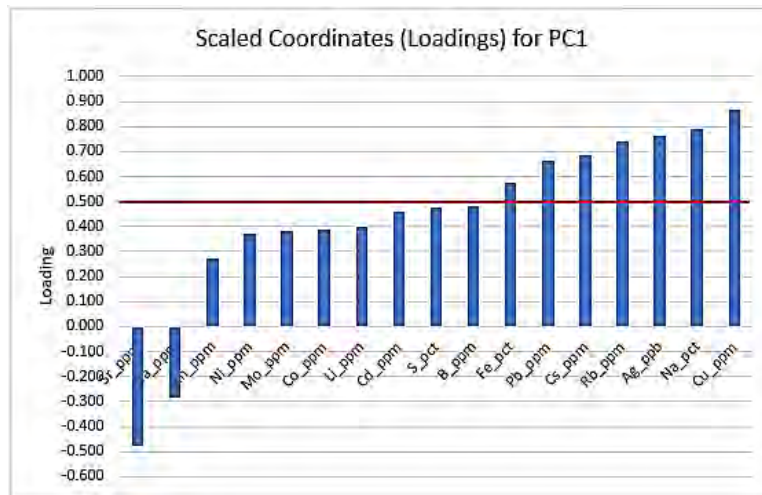


Figure 12. Scaled Coordinates (loadings) for PC1 showing a positive association between Fe, Pb, Cs, Rb, Ag, Na and Cu.

Results

Halogens

Fluorine

Fluorine results (Median: 2.01 ppm) are shown in Figure 13. Concentrations normalized to ash yield (dry equivalent) define a series of anomalies highlighting a distinct north-easterly trend across the map area as well as similar shorter northeast trends and several discrete anomalies located mainly over the Chilcotin Group basalts in the south. The main north-easterly trend

follows the division between predominantly Miocene to Pleistocene-age Chilcotin Group basalts to the southeast and older Tertiary (Ootsa Lake Group) and Mesozoic rocks (Hazelton and Bowser Lakes groups) to the northwest (Figure 13). Diakow and Levson (1997) mapped a north-easterly striking southeast-side down normal fault, which they named the Blackwater fault (shown in bold on Figure 13, on the southeast side of Tsacha Lake), which they interpreted to be the southern boundary of the Nechako uplift: a horst of older rocks forming the Nechako and Fawnie mountain ranges. Angen et al. (2017) dismissed the existence of this fault and concluded, based on aeromagnetic data, that the fault cannot exist because there is no magnetic contrast across the mapped structure suggesting significant offset.

Fluorine results suggest that this fault may indeed exist and furthermore may be part of a more regional structural trend or corridor (referred to here as the Blackwater corridor). The existence of such a corridor is supported by several lines of evidence: a) the F results; b) the abrupt change in bedrock ages from southeast to northwest; and c) magnetic trends identified in the Analytic Signal aeromagnetic image (Figure 14 - Aeroquest, 2014).

Figure 14 shows F results superimposed on the Analytic Signal magnetic image. A corridor of NE-SW orientated lineaments or breaks is apparent (highlighted with white dashed lines). These features are parallel to and extend southwest from the mapped location of the Blackwater fault. Moreover, elevated F concentrations coincide with similar breaks in the southwest and east parts of the map area, possibly highlighting the position of similar structures. North-northwest striking faults that define blocks with contrasting magnetic responses in the central part of the map area do not show any spatial correlation with F.

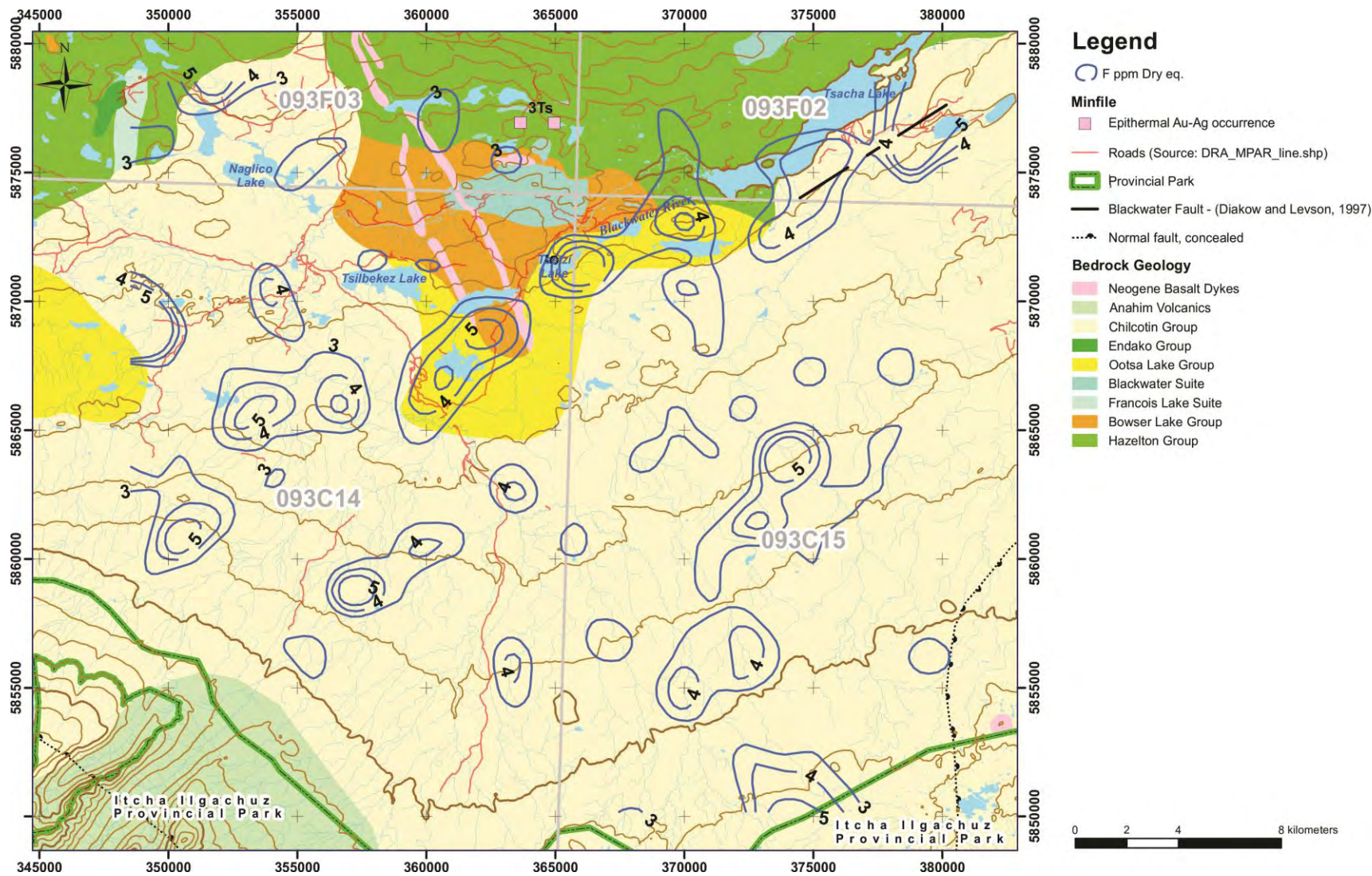


Figure 13. Fluorine (ppm: Dry Equiv.) concentration contours over geology (after Angen et al., 2017).

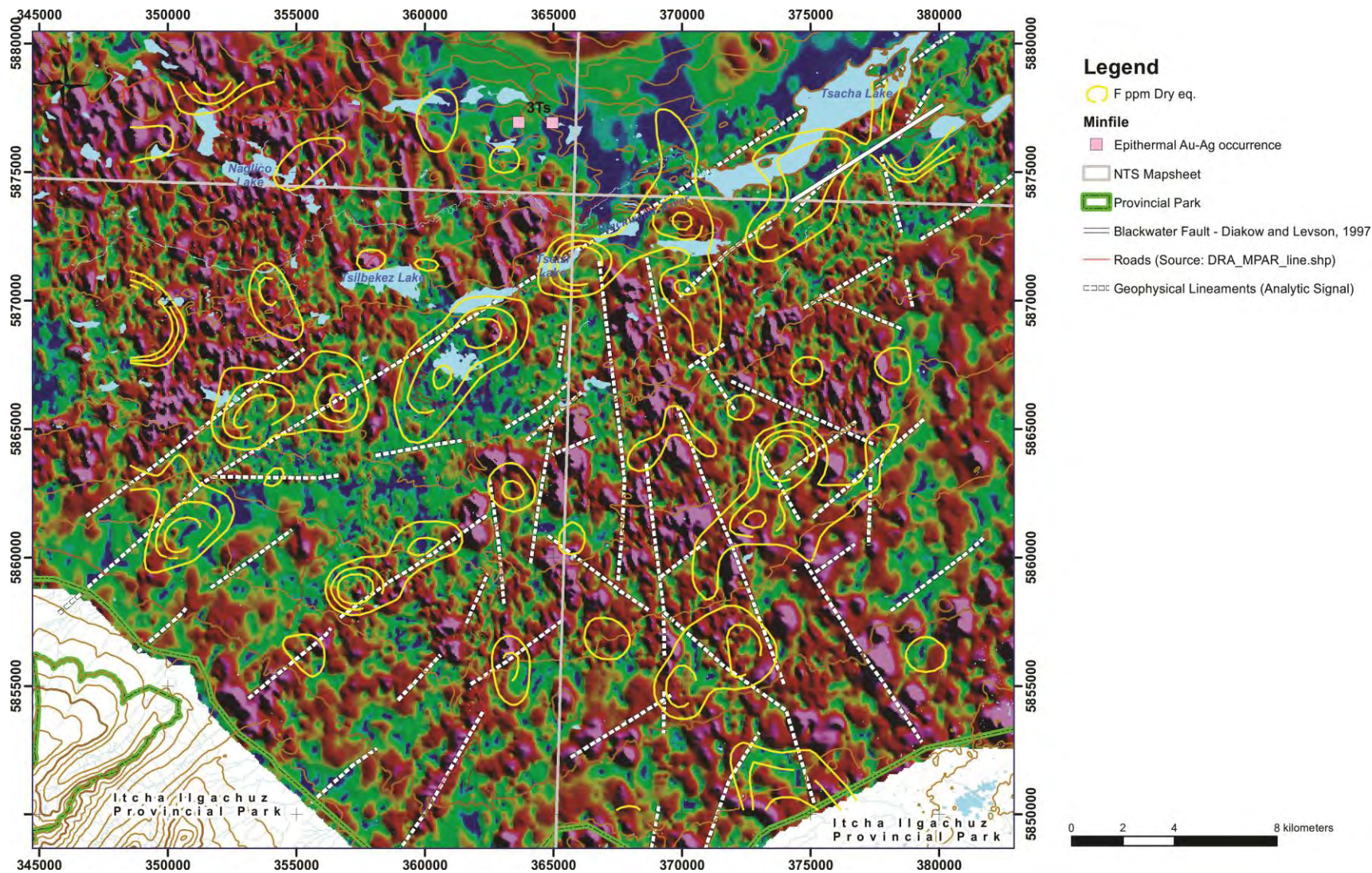


Figure 14. Fluorine ppm dry equivalent contours (yellow) over the Analytic Signal magnetic image (Aeroquest, 2014). Dashed white lines show obvious magnetic breaks that are interpreted to be structures. The mapped Blackwater fault is shown by the solid black line in the NE.

Chlorine

Chlorine results (Median: 19.7 ppm; Figure 15) show three features of interest. The most prominent is a broad ENE-WSW anomalous trend extending from Tsacha Lake to just west of Tsilbekez Lake. The trend lies slightly north of the above-mentioned F trend and has a more ESE-WSW orientation. Highest concentrations overlie mostly Hazelton and Bowser Lake Group rocks but extend into Chilcotin Group at the west end. A second trend aligned NNW-SSE traverses the western part of the map area and is defined by a line of discontinuous anomalies occurring over the Chilcotin Group basalts. There is an indication of a second weaker parallel trend near to the eastern map boundary; however, there are no geological or geophysical explanations for these trends, but a structural cause is likely.

A third area of elevated Cl concentrations is present in the northwest corner of the map area where there is a peninsular of Chilcotin Group basalts extending over Hazelton Group immediately north of Naglico Lake. This feature is not closed off by the sampling coverage. Scattered single point anomalies also occur throughout the central part of the map.

Bromine

Bromine results (Median: 1.48 ppm) are shown in Figure 16. Whereas the Br patterns are more restricted than Cl, they display similar distributions, particularly in the northern part of the map. The most significant feature occurs at the southwest end of Tsacha Lake where an ENE-elongated anomaly coincides with the Cl anomaly and part of the F trend. The axis of this feature follows the northern contact of the Ootsa Lake Group and extends over Bowser Lake and Hazelton Groups to the north. The northern part of the sample grid also shows anomalous concentrations of Br. Here the elevated values are confined to the Hazelton Group; and the anomaly is not closed off by the sampling. Elsewhere, scattered clusters of anomalous samples occur over the Chilcotin Group basalts. The cause of these features is not readily apparent. However, two possible explanations are: 1) anomalous Br values are related to now-eroded eruptive centres (vents or feeder dykes) within the Chilcotin basalts; indeed, some of the anomalies, particularly in the southeast part of the map area appear to occur close to small cinder cones (Google Earth interpretation); and 2) there are unmapped windows of Tertiary and/or Mesozoic basement within the large area mapped as Chilcotin Group.

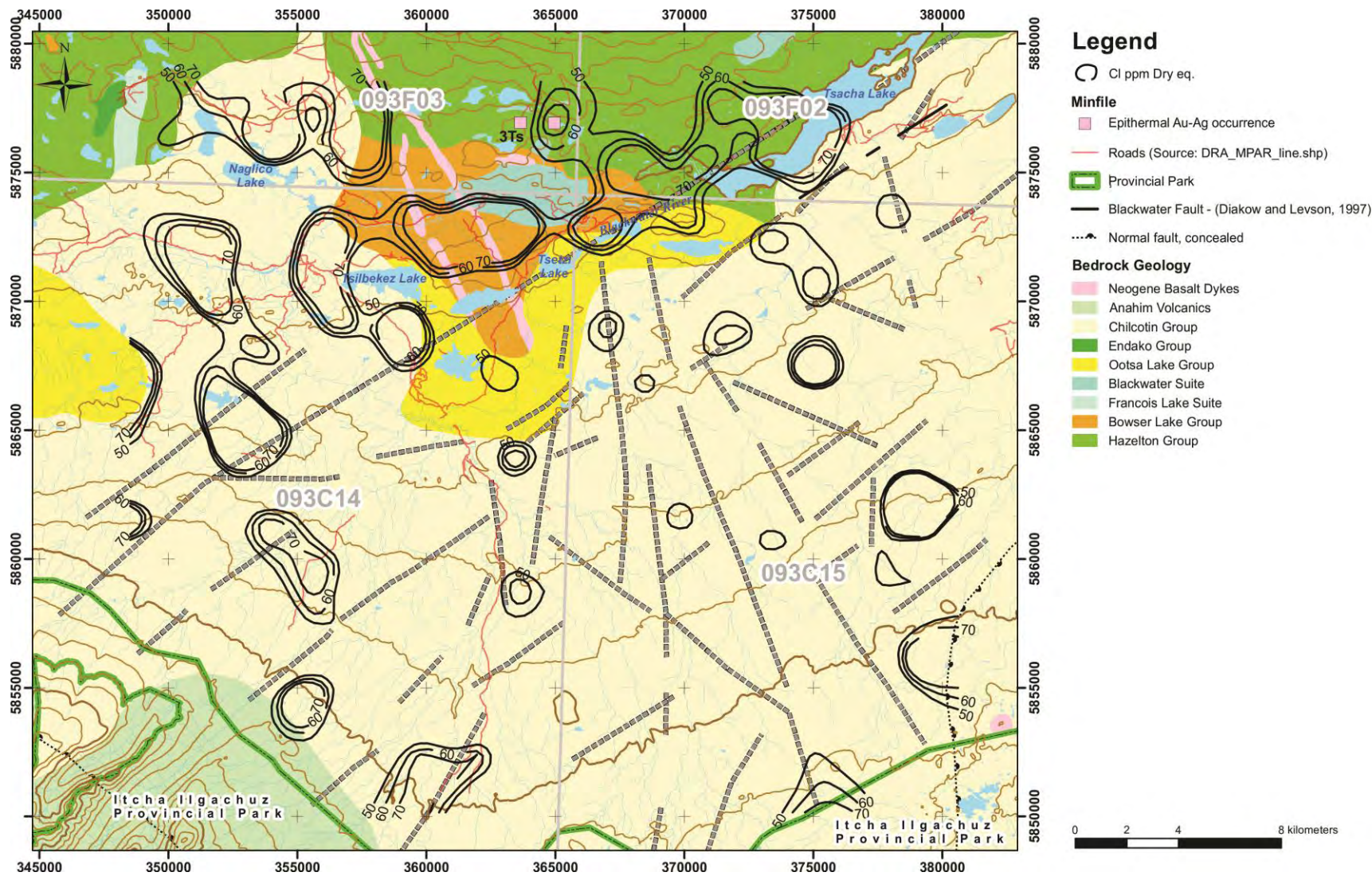
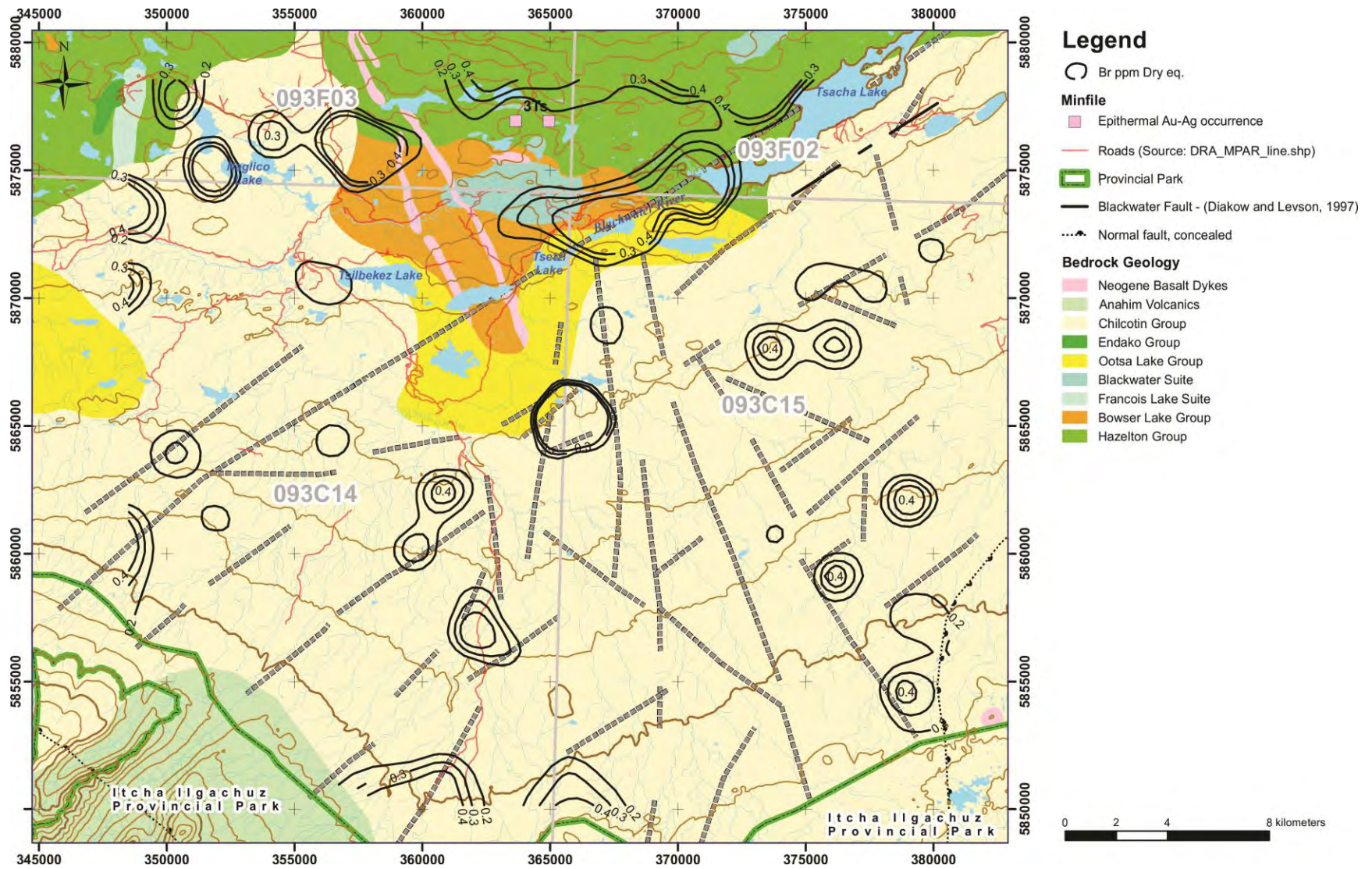
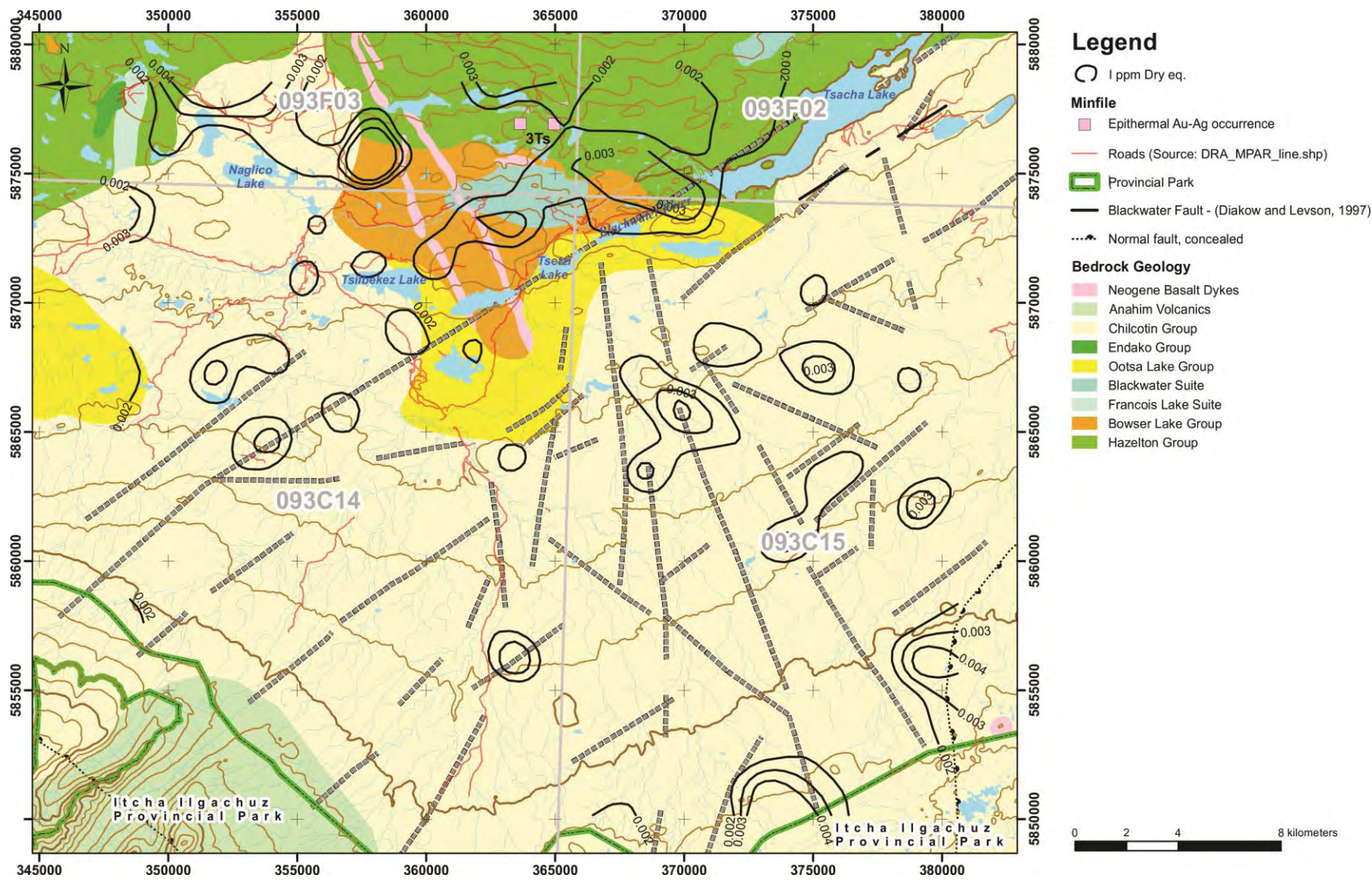


Figure 15. Chlorine ppm dry equivalent contours over regional geology with geophysical lineaments from Figure 14.

Iodine

Iodine concentrations (median: 0.033 ppm) are low and responses are of low contrast. Nevertheless, Figure 17 shows that the patterns are broadly similar to Br and Cl with the most important enrichment occurring on an ENE-WNW trend extending southwest from Tsacha Lake. The axis of this anomaly appears to be displaced to the north of the F, Cl and Br anomalies; it overlies mostly Hazelton and Bowser Lake Groups and the southeast part of the Blackwater Granite (cyan). The area north of Naglico Lake is anomalous and the core of the anomaly correlates well with that highlighted by Br and Cl. In the central and eastern parts of the map area, I enrichments are coincident with those of Cl and Br.





Correlation of halogen anomalies

Box and Whisker plots for Br, Cl and I (Figure 18) show that the major rock units have different background concentrations, : Chilcotin Group basalts (lower values), Ootsa Lake Group, Bowser Lake and Hazelton Groups (higher concentrations). This is important to consider when assessing the importance of elevated concentrations over the Chilcotin basalt covered parts of the study area.

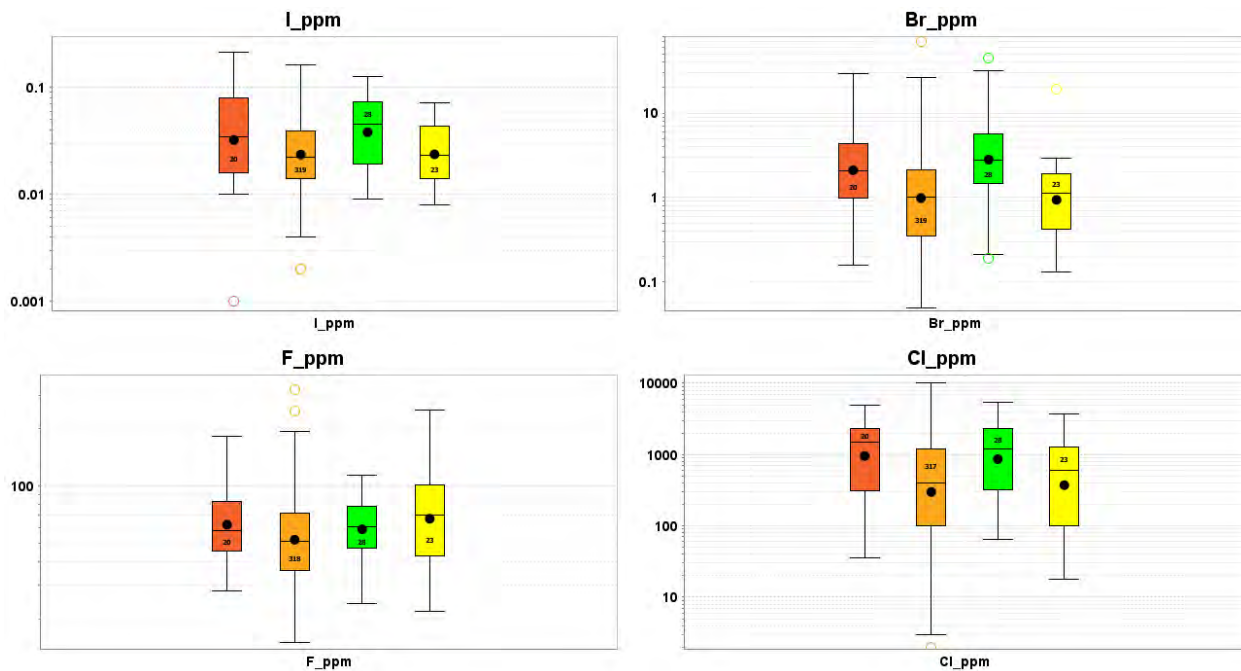


Figure 18. Tukey Box and Whisker Plots showing variations in halogen concentrations in principal geological units.

Figure 19 shows that there are several areas where anomalous concentrations of Cl, Br and I coincide. The most notable occur a) along the east grid margin, in the northeast part of the grid, b) along the northeast trend and c) in the northwest corner of the map area. There are also areas where I correlates with Cl only (i.e. in the west-central part of the map) and on the south boundary near to the southeast corner.

Halogen results show two important relationships: a) a relatively good coincidence of Br, Cl and I anomalies; and b) the relationship between F and inferred northeast structures. To highlight these relationships, Figure 20 shows contour plots of a summative index of Br+Cl+I, and dry equivalent F ppm (red). The index is produced by first log 10 transforming the results and then rescaling them to a range of zero to one, where zero represents the lowest value and one, the highest. Then the rescaled results for Cl, Br and I are summed.

The index values highlight areas where Br, Cl and I anomalies overlap. Figure 20 shows that overlapping patterns of F and the other halogen anomalies are rare. In fact, over most of the grid F displays almost an

antithetic relationship to Cl, Br and I. Fluorine in the southeast two-thirds of the map area appears to highlight northeast-southwest lineaments (inferred from the Analytic Signal magnetic image – dashed lines in Figure 14). The other halogens do not show any compelling relationship to structure.

There are, however, a few areas where anomalies of all four halogens coincide. These are on the west end of the northern grid boundary, on the southeast part of the grid, and on the northeast part of the Blackwater corridor. In the latter area, the overlap is partial because the Br-Cl-I anomaly is slightly displaced to the north.

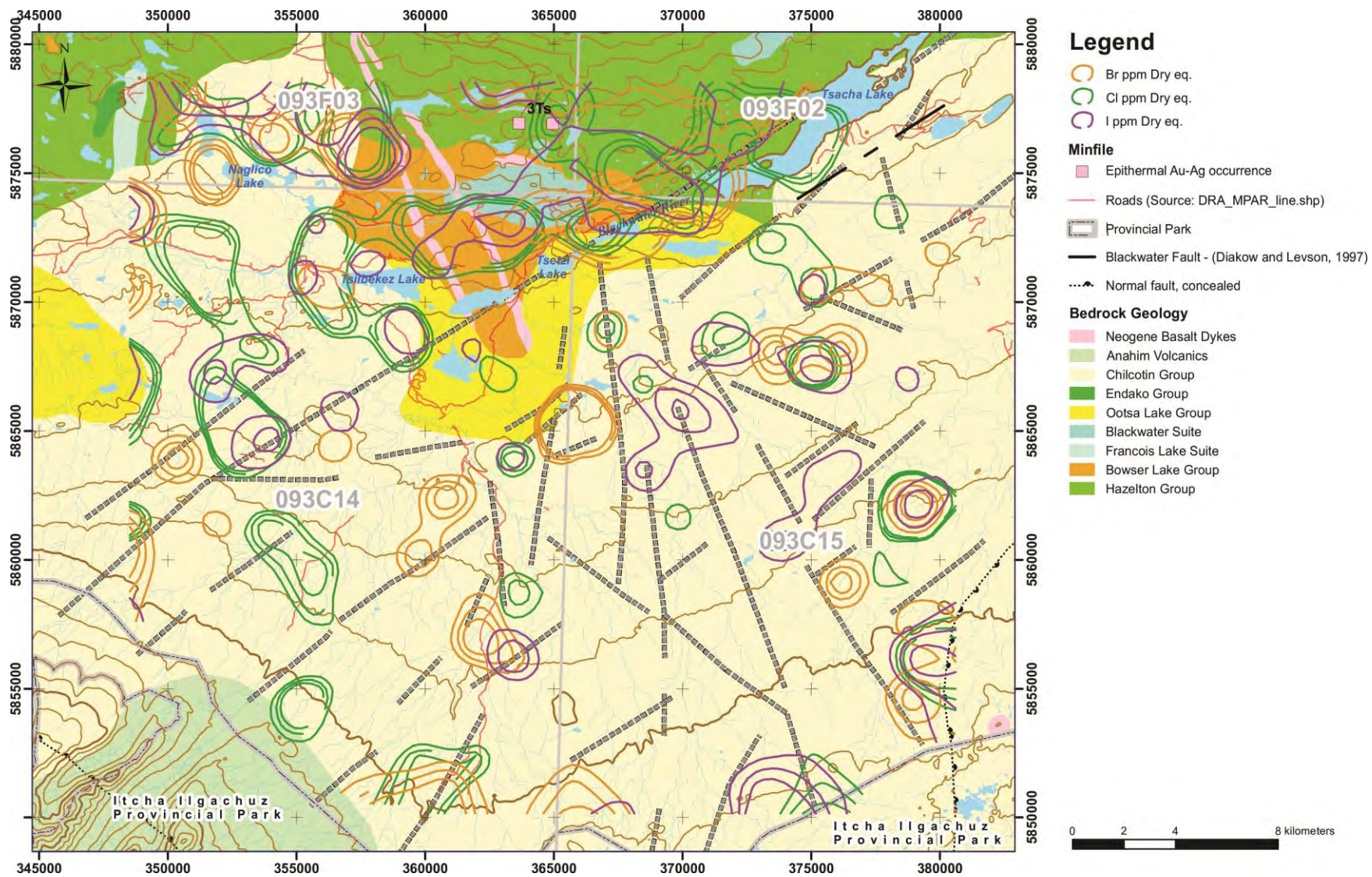


Figure 19. Summary map showing Br, Cl and I anomalies. Geophysical lineaments (dashed black lines) from Figure 14.

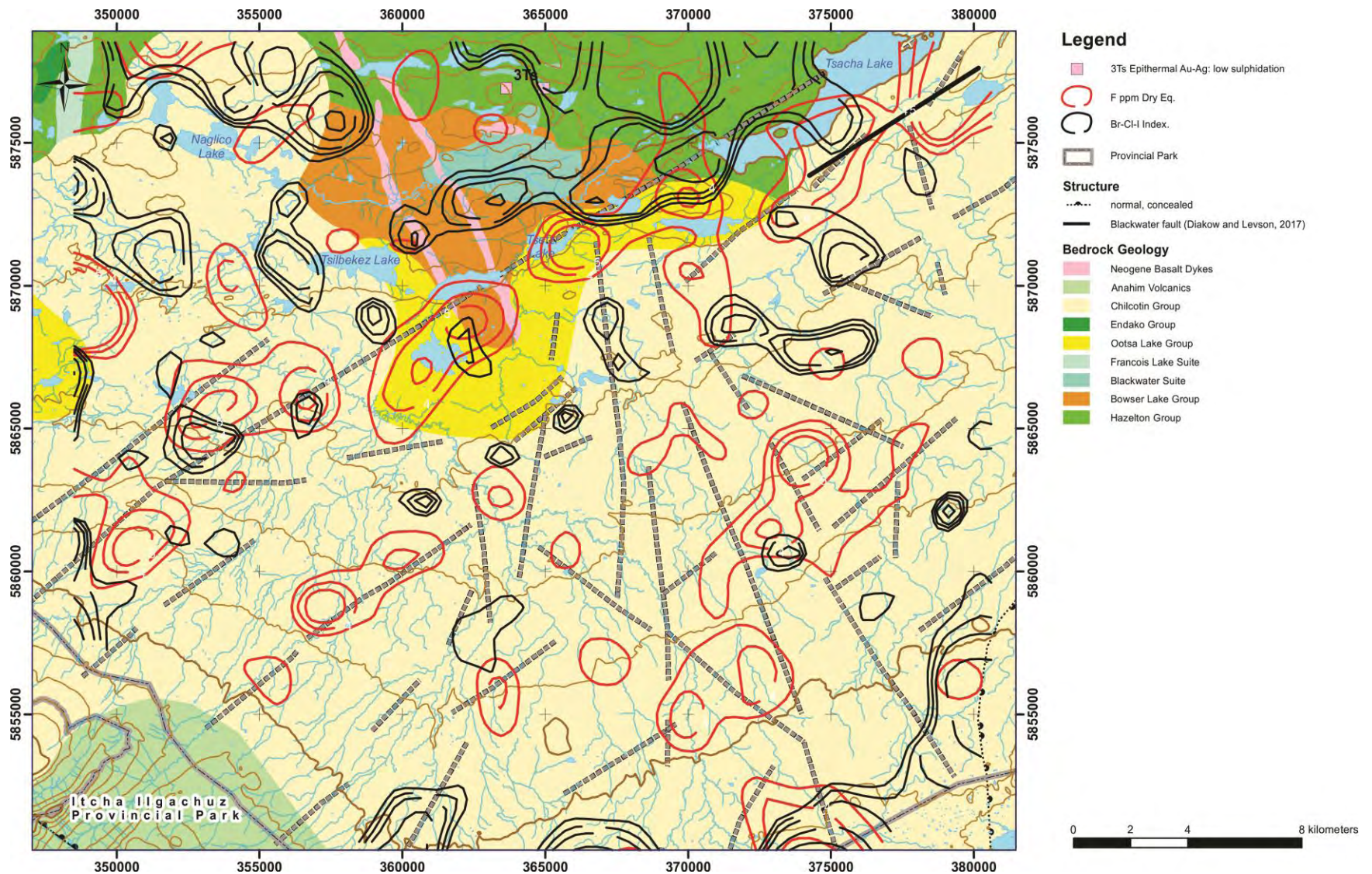


Figure 20. Summary of halogen results showing F ppm dry weight equivalent (red) and contours of a Br-Cl-I summative index (black). The index highlights areas where Cl, Br and I anomalies coincide. Geophysical lineaments (dashed black lines) from Figure 14.

Correlation with pathfinder elements

To investigate the relationship between the halogens and the pathfinder elements, Figure 21 shows a scaled symbol plot of PC1 results (Table 8 and Figure 2) superimposed on the halogen index contours. The map reveals 12 areas where PC1 and the halogen index results coincide. These are indicated by green rectangles labelled A through L. Coincidence of pathfinder element and halogen anomalies is compelling evidence for metal bearing hydrothermal systems. All but two of the features highlighted on Figure 22 occur in areas mapped as Chilcotin Group basalt. Feature L in the north of the sample grid is on Hazelton Group basement rocks and interestingly coincides with the 3Ts epithermal Au-Ag occurrence (Minfile 093F 055 and 093F 068); the only known metal occurrence in the map area. Feature J is near the western boundary of the survey area covering a sliver of Ootsa Lake Group (yellow) captured by the sampling. Feature F is in the NE part of the area and sits adjacent to the mapped segment of the Blackwater fault (Diakow and Levson, 1997). Features A, E, F, H, I all lie within the NE-SW Blackwater fault corridor defined by the aeromagnetic survey.

The most compelling coincident halogen and pathfinder element anomalies are A, B, C and D. Each represents an area of at least 10 km². At feature C, the strongest PC1 values occur in the northern part of the halogen anomaly. At features A and B, strongly anomalous PC1 responses occur over the entire area of the halogen anomalies. Feature D is defined by weaker PC1 responses that are more dispersed than the others anomalies. Each of these areas indicates a possible window through the Chilcotin basalts exposing higher halogen backgrounds typical of the Ootsa Lake and Hazelton groups and as such can be considered as potential targets for epithermal and/or porphyry mineralization beneath the glacial sediment cover. Further investigation of these features is justified.

There are large areas of Br-Cl-I index anomalies without corresponding metal signatures. Conversely, there are PC1 anomalies without halogen responses. Most of the latter comprise single sample anomalies scattered over the southern two thirds of the grid. The most curious feature of these anomalies is that they appear to align along two parallel NW-SE trends. The significance of these trends is not known but potentially they reflect structures beneath the volcanic and glacial sediment cover.

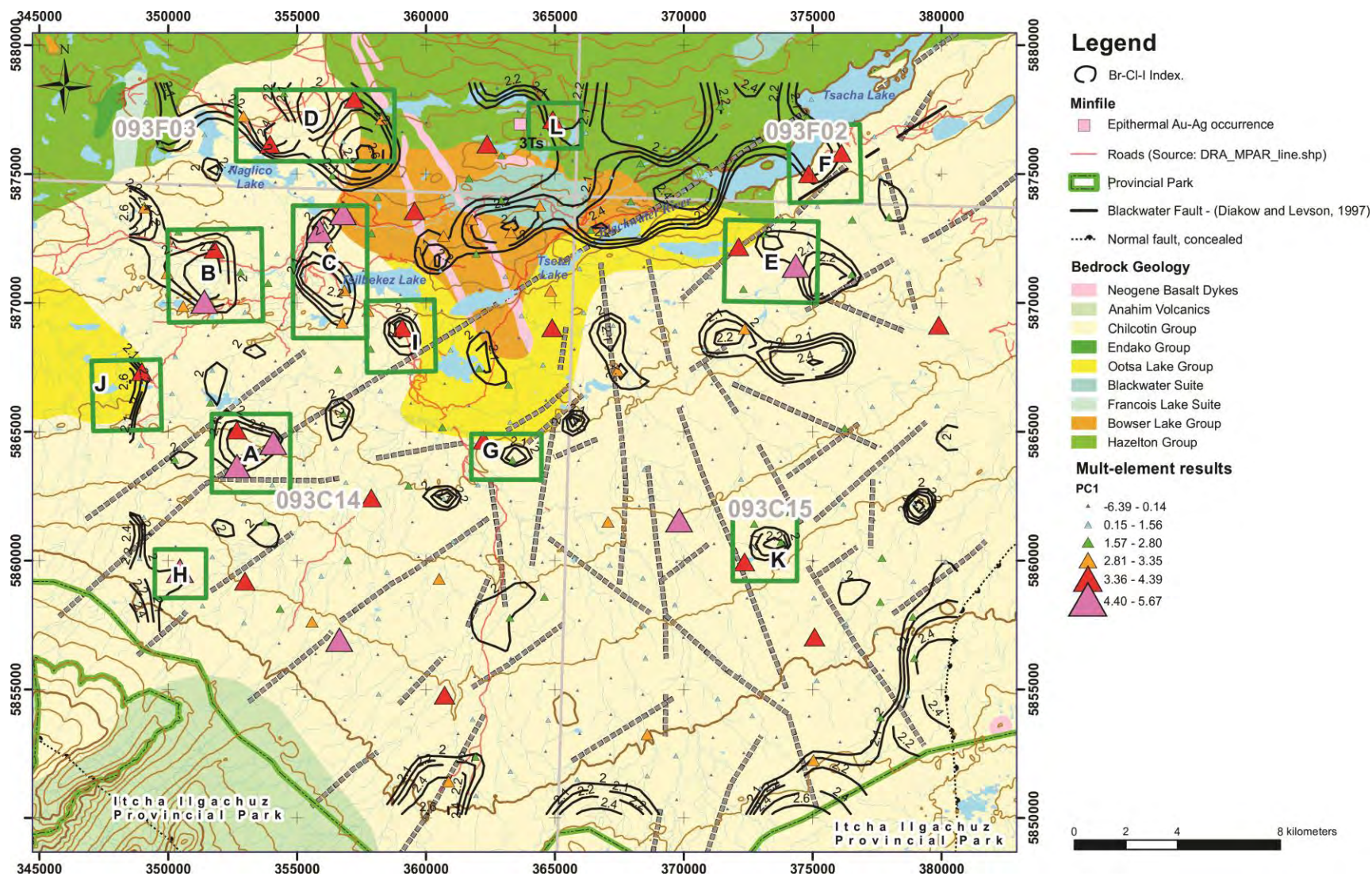


Figure 21. Areas of coincident PC1 scores (progressive half percentile scaled) and halogen index anomalies. Contours indicate halogen index values; grey dashed lines – lineaments from Analytic Signal magnetic image; solid black line – mapped segment of the Blackwater fault (from Diakow and Levson, 1997). Geology after Angen et al., 2017.

Discussion

Diakow and Levson's (1997) observation that the Blackwater fault represents the southern limit of a significant horst block, supports the notion that the fault could be deep-seated. Furthermore, from experimental work, Newton et al. (1998) concluded that concentrated brines (perhaps from volatile-rich alkaline basalts) have high alkali mobility at deep crustal temperatures and therefore could give rise to some element enrichments at the surface – particularly for the highly mobile F along faults and shear zones. With this work in mind, the fact that there is a significant north-easterly trend to the F anomalies that includes the trend of the mapped Blackwater fault (extending beneath cover to the southwest), further supports the concept that this could be a significant fault zone penetrating deeply into the Earth's crust, and acting as a conduit from partial melting at depth for the upward movement of F.

Bromine, Cl and I do not correlate well with F suggesting that the controls on their concentrations in bedrock (and subsequently vegetation) are different. Chlorine, Br and I anomalies appear to form a sub-parallel trend just to the northwest of the main F trend through Tsacha Lake and distinct anomalies distributed throughout the Chilcotin Group.

All three halogens are known to be important ligands for the transport of metals in hydrothermal fluids. Therefore, coincident anomalies of these elements are probably showing areas where there has been some sort of hydrothermal activity involving either magmatically derived fluids (Aiuppa et al., 2009) or meteoric fluids that have interacted with crustal halogen sinks such as evaporites. Evaporites are not known to be present in the Mesozoic or Tertiary basement rocks, therefore that source can be ruled out.

Historically, White Island volcano of New Zealand has been shown to have emitted extraordinarily high Cl-bearing volcanic bombs. They contain glass with up to 1.7% Cl. The F/Cl ratios and their relationship with other constituents show that the F and Cl in the volcanic bombs were derived from hydrothermal fluid, most likely concentrated brine in an active crater pool (Anazawa et al., 2011).

The presence of Br, Cl and I anomalies in vegetation sitting on top of Chilcotin basalt and glacial deposits suggests that the tree roots can access halogen-enriched substrate or ground water derived from it. One source of halogens is potentially the Chilcotin basalts. Halogen enrichment is likely to be present in rocks around eruptive centres such as volcanos, fissures and feeder dykes (cf. Anazawa et al., 2011). This source may explain some of the halogen anomalies without corresponding pathfinder element responses.

The presence of coincident pathfinder and halogen anomalies therefore suggests that the basalts are not the source rocks. They are not known to host metal occurrences. Therefore, the underlying Tertiary and Mesozoic basement are the most likely source for these elements; however, the geology map shows that

most of the sample grid is underlain by Chilcotin Group with no apparent windows of the underlying rocks exposed.

Dohaney (2009) showed that the distribution of the basalt cover is probably significantly over-estimated and noted that un-mapped windows through the basalts exposing potentially mineralization hosting rock units beneath is highly likely. Constraints on the thickness of the Chilcotin Group is discussed by Bordet et al. (2014). Rather than being a uniform sheet of lavas, as implied by the 2017 geology compilation (Angen et al., 2017), the basalts almost certainly ponded in paleo-valleys; the intervening ridges having very thin or no basalt cover. Therefore, the halogen results may be showing areas where the basalts are thin or absent. This in itself is a useful outcome of this work that could direct the focus for more detailed regional mapping of the Chilcotin covered areas. Porphyry and epithermal pathfinder element anomalies in the vegetation can only be explained by metal sources in the sub-Chilcotin stratigraphy, and further field investigation of the anomalies shown in Figure 22 is recommended.

Summary and Conclusions

The following summary and conclusions can be made from the results of this study:

- 1) After reducing vegetation to ash at 475°C for 24 hours, samples were leached with hot de-ionized water (90°C) and the leachate analyzed by a combination of ion chromatography (IC) and inductively-coupled plasma mass spectrometry (ICP-MS). The fine details of the analytical methodology remain proprietary to the commercial laboratory. Optimal aliquot weight proved to be 0.5 g of ash rather than the 0.25 g used previously, based on experimental work by ALS-Geochemistry. No further experimentation has been undertaken to determine halogens in dry tissues since this requires instrumentation not currently available.
- 2) The analytical methods (still under development) produce results with good precision; however, the leach of the ashed sample recovers only the water-soluble fraction. The proportion of the total concentration recovered in the water-soluble fraction remains to be determined.
- 3) Overall precision estimated from field duplicate samples is close to 20% RSD, which is good for reconnaissance samples.
- 4) Anomalous Au values identified in the original multi-element dataset (Jackaman and Sacco, 2016) appear to be confined to one test tube rack that resulted in unrealistically elevated Au concentrations along a segment of one survey line that could not be reproduced. However, it should be noted that the Au values were very low, such that poor precision would likely be expected. The exact nature of this error could not be ascertained by our investigation, but it is likely to be related to digestion time and/or temperature in the laboratory. Reanalyses of those

samples by Bureau Veritas failed to reproduce the anomaly but other anomalous Au values in the north part of the grid did reproduce, although with slightly lower values. Poor reproducibility was also an issue for As, Cr, Ga, Sb and Te. Consequently, all these elements were excluded from this interpretation.

- 5) Halogens produce geologically meaningful patterns in the survey area. Fluorine identifies a northeast striking structural corridor that appears to be aligned with the Blackwater fault proposed by Diakow and Levson (1997). There is strong supporting evidence for a corridor of NE-SW structures in the aeromagnetic results, particularly the Analytic Signal of the total magnetic intensity (GBC Report 2014-04), in contrast to Angen et al.'s (2017) conclusion that the fault is absent.
- 6) Bromine, Cl and I show sympathetic distribution patterns. Elevated concentrations in the northern part of the grid sub-parallel with the Blackwater fault corridor probably indicate background differences between the Hazelton, Bowser Lake and Ootsa Lake Group rocks in the north and Chilcotin basalts to the south.
- 7) Coincident Br-Cl-I index anomalies and PC1 (Ag-Cs-Cu-Fe-Na-Pb-Rb) pathfinder element anomalies suggest areas where magmatic hydrothermal systems may potentially be present. Most occur in the Chilcotin covered part of the survey area, suggesting that they may be highlighting windows through the basalts where porphyry or epithermal style mineralization may occur in the pre-Chilcotin units (e.g. Hazelton and Ootsa Lake groups) beneath.
- 8) The one coincident halogen index and PC1 anomaly on Hazelton Group rocks occurs at the 3Ts epithermal Au-Ag prospect; the only known metal occurrence in the survey area. This confirms that the halogens, in concert with the multi-element geochemistry, can detect the presence of hydrothermal mineralization.

Recommendations

Continued development of the analytical methods is important if the halogen elements are to become widely used by the mineral exploration community. Work should include research into low detection limit methods for determining F in dry organic media, and additional development work of the IC method with the aim of eliminating interferences that affect the F chromatogram peaks in organic-rich media. However, studies should also include assessment of alternative approaches like electro-thermal volatilization-ICP-MS (ETV-ICP-MS) and pyrohydrolysis to further improve analytical precision and direct analysis of dry plant tissues.

Further detailed comparisons of the halogen distribution patterns with the original ICP-MS database (Table A4, Appendix 1) along with consideration of data quality control discussed above, could reveal other interesting associations – e.g. there appears to be a good Cl and Cu association at sites north of the Blackwater fault, but not evident to the south.

Another aspect of future work for improving analytical quality would be the creation and certification of appropriate vegetation control standards. Some suitable controls already exist but they require proper characterization to determine their total and water-soluble halogen contents on both dry and ashed material. Collection and certification of new control samples is also necessary for other common tree and understory species found throughout BC.

A field validation program is recommended to ground-truth the anomalies identified by this study. Field visits should be carried out to coincident halogen index and PC1 anomalies to confirm or refute the presence of unmapped windows of Hazelton or Ootsa Lake Group rocks occurring within the area mapped as Chilcotin basalt and to evaluate them for potential mineralization.

Acknowledgements

We thank Alemayehu Asfaw at ALS–Geochemistry, North Vancouver, for his contributions in developing the analytical technologies used in this study. Initial discussions on this project were with Sarah Rice and Emma Armstrong, and subsequently with Amanda Stoltze, Iyad Al Khatib and other management and staff at ALS who we thank for ongoing discussions and the discounted rate for sample analyses. We are grateful to Wayne Jackaman for discussions on the original sampling program and supplying the ash samples on which this study is based. Finally, we gratefully acknowledge the financial support of Geoscience BC and the province of British Columbia.

References

- Abzalov, M.Z. (2008). Quality Control of Assay Data: A Review of Procedures for Measuring and Monitoring Precision and Accuracy, *Exploration and Mining Geology*, 17(3-4): p. 131-144.
- Aeroquest Airborne Ltd. (2014): Fixed Wing Magnetic Geophysical Survey, TREK Project, Interior Plateau/Nechako Region, British Columbia, Canada; Geoscience BC, Report 2014-04, 40 pp. URL << <http://www.geosciencebc.com/reports/gbcr-2014-04/>>>
- Aiuppa, A., Baker, D.R. and Webster, J.D. (2009): Halogens in volcanic systems: *Chem. Geol.*, v.263, June 15, 2009, p. 1-18. <<<https://doi.org/10.1016/j.chemgeo.2008.10.005>>>
- Al Ajely, K.O., Andrews, M.J. and Fuge, R. (1985): Biogeochemical dispersion patterns associated with porphyry-style mineralization in the Coed Y Brenin forest, North Wales; *in* *Prospecting in Areas of Glaciated Terrain*, Inst. Mining and Metall., London, v. 6, p. 1-10.

- ALS Schedule of Services and Fees, Geochemistry (2020): URL<<<https://www.alsglobal.com/en-ca>
- Anazawa, K., Wood, C. P. and Browne, P.R.L. (2011): Fluorine and chlorine behavior in chlorine-rich volcanic rocks from White Island, New Zealand. *J. of Fluorine Chemistry*, Volume 132, Issue 12, December, p. 1182-1187.
- Angen, J.J., Rahimi, M., Hart, C.J.R., Westberg, E., Logan, J.M. and Kim, R. (2017): Bedrock geology, TREK project area, northern Interior Plateau, central British Columbia; Geoscience BC Map 2017-06-01 and MDRU Map 12-2017, scale 1:250 000. [Download PDF map 10 Mb](#) Map accompanied by GIS files [Download zip file 1.3Gb](#)
- Angen, J. J., Hart, C. J. R., Kim, R. S., and Rahimi, M. (2018): Geology and Mineral Potential of the TREK Area, Northern Interior Plateau, Central British Columbia, Parts of 1:250,000 NTS Sheets 093B, C, F and G; Geoscience BC Report 2018-12, MDRU Publication 411.175 p. URL<<<http://www.geosciencebc.com/major-projects/trek/>>
- Billings, G.K. and Williams, H.H. (1967): Distribution of chlorine in terrestrial rocks: a discussion. *Geochimica et Cosmochimica Acta*, v. 31, p. 22–47.
- Bissig, T, Heberlein D. R. and Dunn, C.E. (2013): Geochemical techniques for detection of blind porphyry copper-gold mineralization under basalt cover, Woodjam Property, South-Central British Columbia (NTS 093A/03, 06). Geoscience BC, Report 2013-17, 54 pp. URL <<http://www.geosciencebc.com/s/Report2013-17.asp>>
- Bordet, E., Mihalynuk, M.G., Hart, C.J.R., and Sanchez, M. (2014): Three-dimensional thickness model for the Eocene volcanic sequence, Chilcotin and Nechako plateaus, central British Columbia (NTS 092O, P, 093A, B, C, E, F, G, K, L); in Geoscience BC Summary of Activities 2013, Geoscience BC, Report 2014-1, p. 43–52.
- Cook, S.J. and Jackaman W. (1994): Regional lake sediment geochemistry and water geochemistry of part the Nechako River map area (93F/2.3: Parts of 93F/6,11,12,13,14). British Columbia Ministry of Mines and Petroleum Resources, Open File 1994-19.
- Cope, G.R. and Spence, C.D. (1995): Mac porphyry molybdenum prospect, north-central British Columbia; in *Porphyry deposits of the northwestern Cordillera of North America*; Special Volume 46, CIMM, p. 757-763.
- Diakow, L. J. and Levson V.M. (1997): Bedrock and Surficial Geology of the Southern Nechako Plateau, Central British Columbia, Ministry of Employment and Investment, Geoscience Map, 1997-2, 1:100,000 Scale.

- Dohaney, J.A.M. (2009): Distribution of the Chilcotin Group basalts, British Columbia: Unpublished M.Sc. Thesis, The University of British Columbia, Faculty of Graduate Studies, August 2009, 136 pp. URL <<<https://open.library.ubc.ca/cIRcle/collections/ubctheses/24/items/1.0052663>>>
- Dostal, J., Hamilton T. S. and Church, B. N. (1996): The Chilcotin basalts, British Columbia (Canada): Geochemistry, petrogenesis and tectonic significance. - N. Jb. Miner. Abh. V. 170, p. 207 -229.
- Dunn, C.E. (1995): Biogeochemical prospecting in drift-covered terrain of British Columbia; in Drift Exploration in the Canadian Cordillera, P.T. Bobrowsky, S.J. Sibbick, J.M. Newell and P.F. Matysek (ed.), BC Ministry of Energy and Mines, Paper 1995-2, p. 229-238, URL<<<http://www.empr.gov.bc.ca/Mining/Geoscience/PublicationsCatalogue/Papers/Pages/1995-2.aspx>>>
- Dunn, C.E. (2007): Biogeochemistry in Mineral Exploration, (Handbook of Exploration and Environmental Geochemistry 9, Series editor, M. Hale), Elsevier, Amsterdam, 462 pp.
- Dunn, C.E., Cook, S.J. and Hall, G.E.M (2007): Final Report for Geoscience BC Project 2005-008 Halogens in Surface Exploration Geochemistry: Evaluation and Development of Methods for Detecting Buried Mineral Deposits. Geoscience BC Report 2007-10, 74 pp. URL <<<http://www.geosciencebc.com/s/2007-10.asp>>>
- Giles, T.R. and Levson, V.M. (1995) Surficial geology and Quaternary Stratigraphy of the Tsacha Lake area, NTS 93F/2; British Columbia Ministry of Energy Mines and Petroleum Resources, Open File 1995-10 (1:50,000 map).
- Heberlein, D.R., Dunn, C.E. and Rice, S. (2017a): Halogens and other volatile compounds in surface sample media as indicators of mineralization, part 1: Lara VMS deposit, Vancouver Island (NTS 092B13); Geoscience BC Report 2017-11, 42 po., CD, URL <http://www.geosciencebc.com/i/project_data/GBCReport2017-11/GBCR2017-11_Lara_Rpt.pdf> [September 2019].
- Heberlein, D.R., Dunn, C E. and Rice, S. (2017b): Halogens and other volatile compounds in surface sample media as indicators of mineralization, part 2: Mount Washington epithermal Au-Cu-Ag prospect, Vancouver Island (NTS 092F/14); Geoscience BC Report 2017-12, 61 pp., CD, URL <http://www.geosciencebc.com/i/project_data/GBCReport2017-12/GBCR2017-12_MW_Rpt.pdf> [November 2019]
- Jackaman, W. and Sacco, D.A. (2016): Reconnaissance biogeochemical survey using spruce-tops in the West Road (Blackwater) River area, Fraser Plateau, British Columbia; Geoscience BC, Report

2016-05, 8pp. + 3 appendices. URL <http://www.geosciencebc.com/reports/gbcr-2016-05/> [September 2019].

Kendrick, M.A. and Burnard, P. (2013): Noble Gases and Halogens in Fluid Inclusions: A Journey Through the Earth's Crust; *in* The Noble Gases as Chemical Tracers, Advances in Isotope Geochemistry, 2013, p. 319-369.

Kendrick, M.A., Woodhead, J.D. and Kamenetsky, V.S. (2012): Tracking Halogens through the Subduction Cycle. *Geology*, December 2012; v. 40; no. 12; p. 1075–1078.

Lavery, N.G. (1985): The use of fluorine as a pathfinder for volcanic-hosted massive sulfide deposits. *J. Geochem. Explor.*, v23, Issue 1, p.35-60.

Lee, D.H., Kwon, S.H., Kim, S.H., Lee, S.H. and Min, B. (2006). Determination of Halogen Elements in Volatile Organohalogen Compounds by the Wickbold Combustion Pretreatment Method and Ion Chromatography. *Bull. Korean Chem. Soc.* 2007, Vol. 28, No. 1, p. 59-62.

Levson, V.M. and Giles, T.R. (1997): Quaternary Geology and Till Geochemistry Studies in the Nechako and Fraser Plateaus, Central British Columbia (93C/1, 8, 9, 10; F/2, 3, 7; L16; M/1). *In* Interior Plateau Geoscience Project: Summary of Geological, Geochemical and Geophysical Studies (Eds. L.J. Diakow, J.M. Newell and P. Metcalfe). Geological Survey of Canada OF3448 and BC Geological Survey Branch Paper 1997-2.

Newton, R.C., Aranovich, Ya., Hansen, E.C. and Vandenheuvel, B.A. (1998): Hypersaline fluids in Precambrian deep-crustal metamorphism. *Precambrian Research*, V.91, Issues 1–2, p. 41-63. [https://doi.org/10.1016/S0301-9268\(98\)00038-2](https://doi.org/10.1016/S0301-9268(98)00038-2)

Ryder, J.M. and Clague, J.J. (1989): British Columbia Quaternary stratigraphy and history, Cordilleran Ice Sheet. *In* Quaternary Geology of Canada and Greenland. Edited by R.J. Fulton. Geological Survey of Canada, Geology of Canada, no. 1, p. 48-58.

Sacco, D., Arnold, H., Ferbey, T. and Jackaman, W. (2017a): Basal till potential of the Carnlick Creek map area (NTS 093C/14), British Columbia: BC Geological Survey Open File 2017-06 and Geoscience BC map 2017-02-05. URL << <http://www.geosciencebc.com/major-projects/trek/>>>

Sacco, D., Arnold, H., Ferbey, T. and Jackaman, W. (2017b): Basal till potential of the Kushya River map area (NTS 093C/15), British Columbia: BC Geological Survey Open File 2017-07 and Geoscience BC map 2017-02-06. URL << <http://www.geosciencebc.com/major-projects/trek/>>>

Seedorff, E. and Einaudi, M.T. (2004): Henderson Porphyry Molybdenum System, Colorado: I. Sequence and Abundance of Hydrothermal Mineral Assemblages, Flow Paths of Evolving Fluids, and

Evolutionary Style: Econ. Geol. V. 99, pp. 3-37. Sweester, P.B. (1956): Decomposition of organic fluorine compounds by Wickbold oxyhydrogen flame combustion method. Anal. Chem., 28, 11, 1766-1768.

Tipper, H.W. (1971): Glacial geomorphology and Pleistocene history of Central British Columbia. Geological Survey of Canada, Bulletin 196, 89 pp.

Trofimov, N.N. and Rychkov A.I. (2004): Iodine and Bromine: Geochemical Indicators of Deep Ore Deposits: Translated by Dr. Edward Erlich & Mrs. Mary-Margaret Coates. Colorado Mountain Publishing House, Denver, Colorado, 205 pp.